iScience

CellPress
OPEN ACCESS

Article

Single-cell transcriptomic reveals a cell atlas and diversity of chicken amygdala responded to social hierarchy

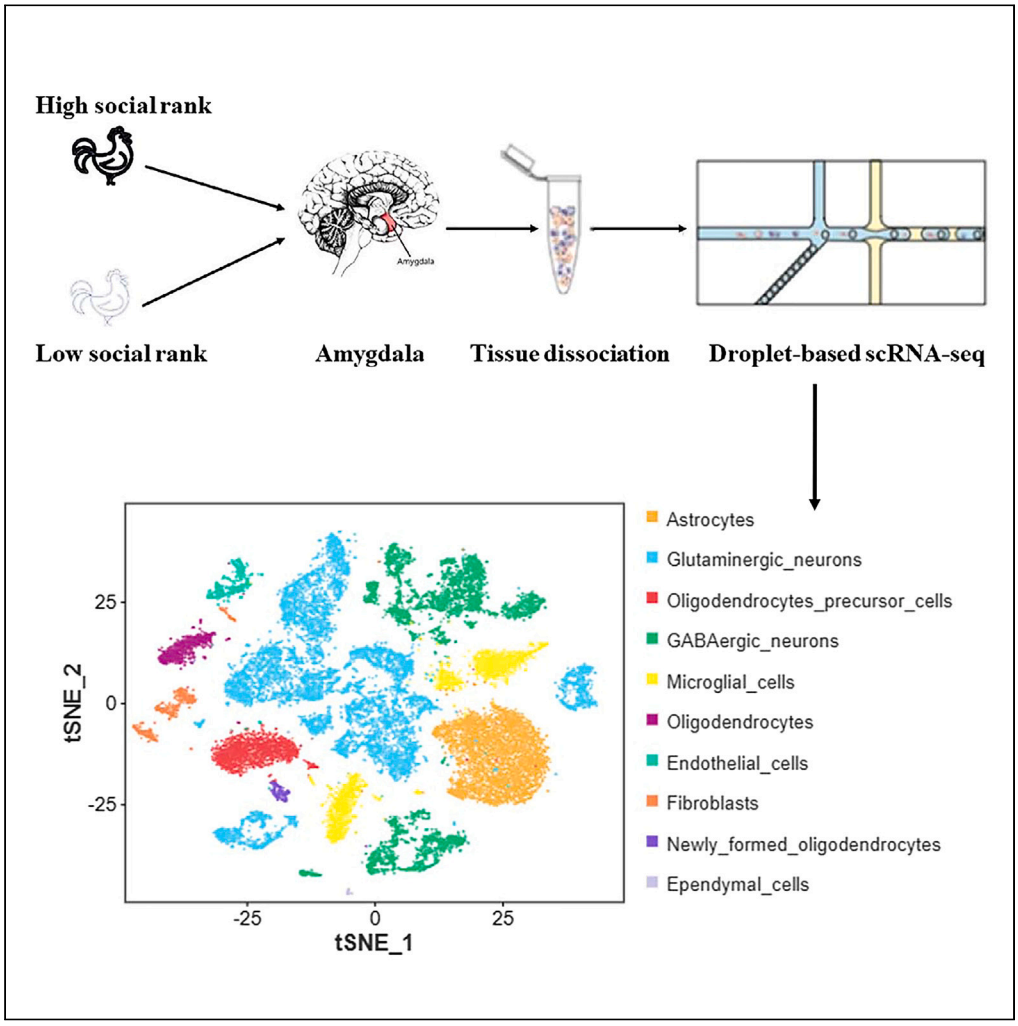

Siyu Chen, Limin Xing, Zhijiang Xie, ..., Haiquan Zhao, Zheng Ma, Hua Li

chensiyu@fosu.edu.cn (S.C.)
mz8522@163.com (Z.M.)
okhuali@fosu.edu.cn (H.L.)

Highlights

We obtain a comprehensive cellular atlas of the domestic chicken amygdala cell type

We performed found out that cell types of human and rhesus monkeys were more closely related and that of chickens were more distant from them

We identified 26 clusters including two neurons and eight non-neurons clusters. Of which, the GABAergic and glutamatergic neurons are considered as main neurons mediating the social hierarchy in chickens

RHOB and *CDK14* might be involved with the role of the mechanism of social hierarchy in chickens

Chen et al., iScience *27*, 109880
June 21, 2024
https://doi.org/10.1016/j.isci.2024.109880

iScience

CellPress
OPEN ACCESS

Article

Single-cell transcriptomic reveals a cell atlas and diversity of chicken amygdala responded to social hierarchy

Siyu Chen,[1,3,4,*] Limin Xing,[1,3] Zhijiang Xie,[1] Mengqiao Zhao,[1] Hui Yu,[1] Jiankang Gan,[2] Haiquan Zhao,[1] Zheng Ma,[1,*] and Hua Li[1,2,*]

SUMMARY

Amygdala serves as a highly cellular, heterogeneous brain region containing excitatory and inhibitory neurons and is involved in the dopamine and serotoninergic neuron systems. An increasing number of studies have revealed the underpinned mechanism mediating social hierarchy in mammal and vertebrate, however, there are rare studies conducted on how amygdala on social hierarchy in poultry. In this study, we conducted food competition tests and determined the social hierarchy of the rooster. We performed cross-species analysis with mammalian amygdala, and found that cell types of human and rhesus monkeys were more closely related and that of chickens were more distant. We identified 26 clusters and divided them into 10 main clusters, of which GABAergic and glutamatergic neurons were associated with social behaviors. In conclusion, our results provide to serve the developmental studies of the amygdala neuron system and new insights into the underpinned mechanism of social hierarchy in roosters.

INTRODUCTION

The amygdala is a highly cellular, heterogeneous brain region that contains excitatory and inhibitory neurons and various nonneuronal cell types as well.[1] Neuronal transcription is closely related to changes in the structure and function of neurons.[2] The amygdala is known for controlling emotion and social behaviors, learning, and is involved in the dopamine and serotoninergic neuron systems and closely related to social hierarchy of animals,[1] and therefore as a targeted brain organ/used to identify the neuron diversity in response to social behaviors. The highest ranking macaque has bilateral amygdala damage, which will reduce social status, while the competitiveness of low ranking individuals increases in the transition to authoritarian rule.[3] In addition, the activation of $GABA_A$ receptors in the basolateral amygdala will prevent hamsters from failing to acquire conditions, thereby affecting social hierarchy.[4] In relation to social hierarchy, extensive knowledge is accumulated on how social status influences brain function and health to understand the neural mechanisms that underlie dominance behavior. In mice, the epigenetic regulation of winning experience was responsible for the ascendance in social status[5] and, further, a novel pathway of lncRNA AtLAS and its target syn2b were revealed in the regulation of social hierarchy by controlling postsynaptic AMPAR trafficking.[6] In macaques, social hierarchy was found to be associated with the immune function and was regulated by the toll-like receptor 4 pathway.[7] In mammals, accelerated evolution of an Lhx2 enhancer PAS1-Lhx2 modulates social hierarchy and was essential for establishing social stratification.[8] Additionally, in ants, the Kr-h1 was known to maintain distinct caste-specific neurotranscriptomes in response to socially regulated hormones.[9] However, there are rare studies conducted on the interaction of amygdala function on social hierarchy in avians.

On the other hand, single-cell RNA sequencing (scRNA-seq) enables the identification of cell subtypes and elucidation of single-cell transcriptomic dynamics.[10] The scRNA-seq is a particularly powerful tool for locating target cells of neuronal neurons, as it allows effective analysis of related mRNAs and host signature genes in a single cell,[11] and can provide an unbiased characterization of behavior-host interactions in individual cells, which are ignored at the population level.[11] Recently, scRNA-seq has made significant research progress in different brain tissues. For example, scRNA-seq revealed the diversity of mouse hypothalamic cells and found that food deprivation had different transcriptional effects between different neuronal subtypes,[12] as well as cell type and the transcriptional of mouse amygdala response to fear conditioning.[13]

Significantly, scRNA-seq was also used to generate a cell atlas of the chick retina,[14] limb,[15] and skeletal muscles,[16] develop an intricate interplay between cellular differentiation and morphogenesis of chicken heart,[17] and gonadal sex differentiation in the chicken embryo.[18] However, the complete classification of cell types in amygdala of chicken has not been reported. Study the network of specialized neuronal

[1]Guangdong Provincial Key Laboratory of Animal Molecular Design and Precise Breeding, Key Laboratory of Animal Molecular Design and Precise Breeding of Guangdong Higher Education Institutes, School of Life Science and Engineering, Foshan University, Foshan 528250, China
[2]Guangdong Tinoo's FOODS Group Co., Ltd, Qingyuan 511500, China
[3]These authors contributed equally
[4]Lead contact
*Correspondence: chensiyu@fosu.edu.cn (S.C.), mz8522@163.com (Z.M.), okhuali@fosu.edu.cn (H.L.)
https://doi.org/10.1016/j.isci.2024.109880

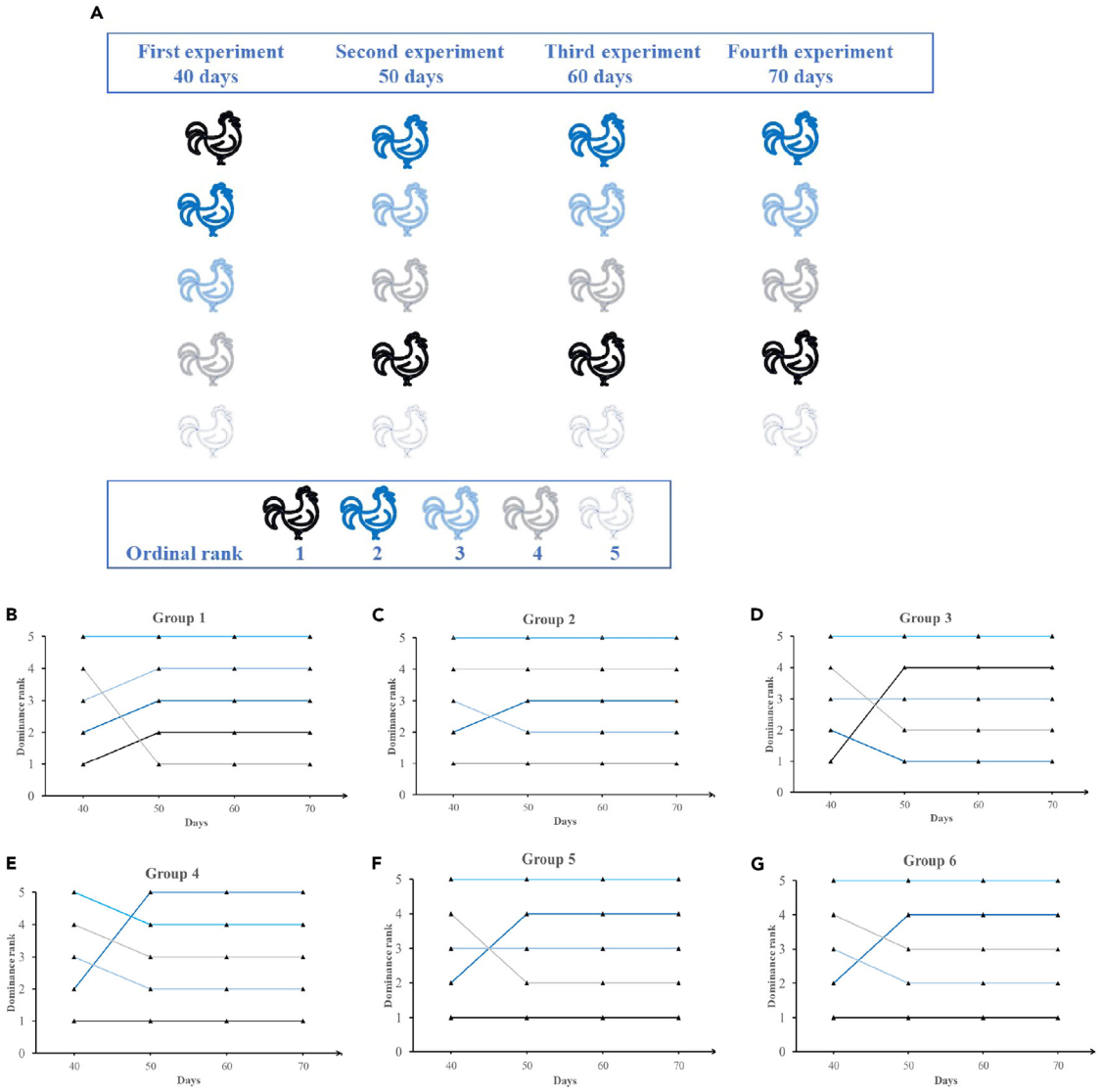

Figure 1. Results of the social hierarchy for roosters

(A) Social hierarchy of roosters at different age. Each row represents a rooster, and different colors represent different social ranks.

(B–G) Represent the social hierarchy results of groups 1 to 6, respectively. The horizontal axis represents the age of roosters, the vertical axis represents social hierarchy, lines of the same color connected represent a rooster.

and glial cell types of chicken brain, and how it plays a role in the establishment of social hierarchy, in order to better understand the underpinned mechanism by which brain neurons on social behaviors. In this study, we established social hierarchies by food competitive tests in roosters, and profiled the deep transcriptomes of amygdala cells from highest and lowest social rank roosters. We determined the transcriptional profiles of amygdala cells to figure out different subtypes of neurons at different social hierarchies exhibit different transcriptional effects. Our results will provide a cellular reference map of the amygdala and lead to discover new potential social behavior foundations for future selection strategy for breeders.

RESULTS

Overview of the cell types in the amygdala identified by scRNA-seq

In order to explore the characteristics of cell transcriptome of amygdala, we used amygdala tissue of roosters for scRNA-seq. We ranked each group of chickens in terms of the aggressive interactions determined by four food competition tests, and the results showed that the social rank of chickens tended to stabilize along as they age (Figure 1). In order to evaluate the influence of social hierarchy on cell type of amygdala, scRNA-seq was conducted in amygdala of chickens with high and low social ranks.

Cells with less than 400 genes or more than 10% mitochondrial unique molecular identifier (UMI) counts were filtered out, and only genes with at least one UMI count detected in at least one cell were used for further analysis. The sequencing data statistics and quality control were shown in Table S1. After removing cells with minimum and maximum thresholds for read numbers per cell (nUMI), number of genes detected per cell (nGene), and mitochondrial RNA genes were determined. There were 14672 and 11753 estimated cells in the high social rank (HSR) and the low social rank (LSR) roosters, respectively (Table S1). After removing low-quality cells, batch effect correction was calculated. First, canonical correlation analysis (CCA) was performed on all samples and then the mutual nearest neighbors (MNN) between cells was found to construct the correspondence between cells. Finally, multiple samples used the correspondence between cells as anchors to complete data integration and batch effect correction.[19]

Classification of cell types in amygdala

Cell types were classified based on t-distributed Stochastic Neighbor Embedding (tSNE) dimensionality reduction and unsupervised cell clustering. Accordingly, 26 cell clusters were identified based on the expressed unique transcriptional profiles (Figure 2B). The information of these cell types was shown in Table S2. We further divided them into eight main clusters including GABAergic neurons, glutaminergic neurons, astrocytes, oligodendrocytes, oligodendrocytes precursor cells (OPCs), newly formed oligodendrocytes (NFO) ependymal cells, endothelial cells, microglial cells, and fibroblasts (Figure 2C). We defined each cluster by the expression of specific marker genes (Figures 2D–2K). The GABAergic neurons were marked by *gad1*, *gad2*, *nrxn3*, and *slc32a1*; the glutaminergic neurons were defined by *slc17a6*, *lmo3* and *gls2*; the oligodendrocyte was identified by *cnp* and *ugt8*; the OPC were marked by *pdgfra* and *myt1*; and the NFO were defined by *fyn*. These cell subtypes reflected various differentiation stages of oligodendrocytes. The astrocytes could also be distinguished from subtype markers *gja1*, *aqp4* and *acsbg1*. The endothelial were marked by *flt1*, *egfl7* and *eng*. We identified microglial cells through four marker genes *sall1*, *sncb*, *tmsb4x* and *fth1*. The expression of *prdm6* and *bnc2* represented fibroblasts. The ependymal cells were marked by *spef2*. The expression of each gene in the subpopulation ia shown in Figure S1. Overall, the types of clusters in this study were similar to those in brain regions of other species.[20]

The amygdala harbors multiple transcriptionally distinct neuron subtypes

We identified eight glutamatergic neuron subtypes, and six GABAergic neuron subtypes. After that, 5054 GABAergic neurons were divided into 12 sub-clusters (Figure 3A), and 10475 glutamatergic neurons were into 13 sub-clusters (Figure 3B) by tSNE. *Slc32a1* was the essential marker genes of GABAergic neurons,[21] which was highly expressed in all 12 neuronal sub-clusters (Figure S2A). Generally, *slc17a6* (*vglut2*) and *slc17a7* (*vglut1*) were central marker genes for glutamatergic neuron.[21] In this study, we found that *slc17a6* was expressed in each sub-cluster (Figure S2B), but *slc17a7* was not detected. To further identify the differential genes of each cell sub-clusters, we generated transcriptome heatmaps of the top five up-regulated genes in each sub-cluster (Figures 3C and 3D). After that, we performed cell set up-regulated gene analysis on glutamatergic and GABAergic neuron. In glutamatergic neuron, there were 520, 562 and 517 up-regulated genes in the sub-clusters 5, 10 and 11, respectively (Figure S2C). GABAergic neuron had 595 genes up-regulated in sub-cluster 9 and 564 genes up-regulated in sub-cluster 11 (Figure S2D).

Analysis classes of GABAergic neurons in amygdala

In order to further classify GABAergic neurons, medial ganglionic eminence (MGE-class neuron; cluster 1,5,6,9), caudal ganglionic eminence (CGE-class neuron; cluster: 7,11), and lateral ganglionic eminence (LGE-class neuron; cluster: 0,2,3,4,8,10) were obtained according to a previous study[22] (Figure 4A). MGE-class neuron significantly expressed SST cortical interneurons, including *sst*, *sox6* and *trps1*. Moreover, the typical interneuron genes *lamp5* and *maf* were highly expressed in MGE-class neuron. The cell cluster in MGE-class neuron was similar to that of SST cortical interneurons. CGE-class neuron significantly expressed genes *prox1*, *adarb2*, and *cnr1*, which were enriched in cortical interneurons, indicating that these cells are similar to CGE-class neuron derived cortical interneurons in transcription.[23] In contrast, LGE was identified by marker genes *tshzi1*, *pbx3*, *meis2*, and *zehx4*, which were mainly expressed in olfactory bulb interneurons in mouse and human.[24] The expression of each gene in the subpopulation was shown in Figure 4B. We used monocle analysis to reconstruct the differentiation relationship of sub-clusters. A total of 12 sub-clusters showed three different developmental trajectories, indicating different origins and destinations of GABAergic neurons in the amygdala (Figure 4C). We determined the development starting point according to the gene expression of *lhx6* in GABAergic neurons progenitor cells (Figure 4D). It can be seen from the Figure 4D that GABAergic neurons mainly have two different development tracks.

Glutamatergic neurons diversity in amygdala

We then described the known and new populations emerging from the classification. Based on unsupervised clusters and transcriptional analysis, we revealed four different glutamatergic neurons subgroups, which were called glu.1 (cluster 5,10,11), glu.2 (cluster 0,1,2,7,8,9,12), glu.3 (cluster 4,6), and glu.4 (cluster 3) (Figure S3A). Glu.1 cells were enriched the marker genes, *xylt1*, *gabrg3*, *zbed1*, *nts* and *col12a1*; glu.2 was clustered by the expression of *slit3*, *il1rapl2*, *grm1*, *sorcs2*, and so on; *snx9* and *znf385b* were co-expressed in glu.3 (sub-cluster 4 and 6); and *nkain3* was the top differential marker gene of glu.4 (Figure S3B). Similarly, for the monocle analysis of 13 glutamatergic neurons, the results showed four differentiation directions (Figure S3C). However, the origin of the differentiation was not identified by the marker genes of the glutamatergic progenitors.

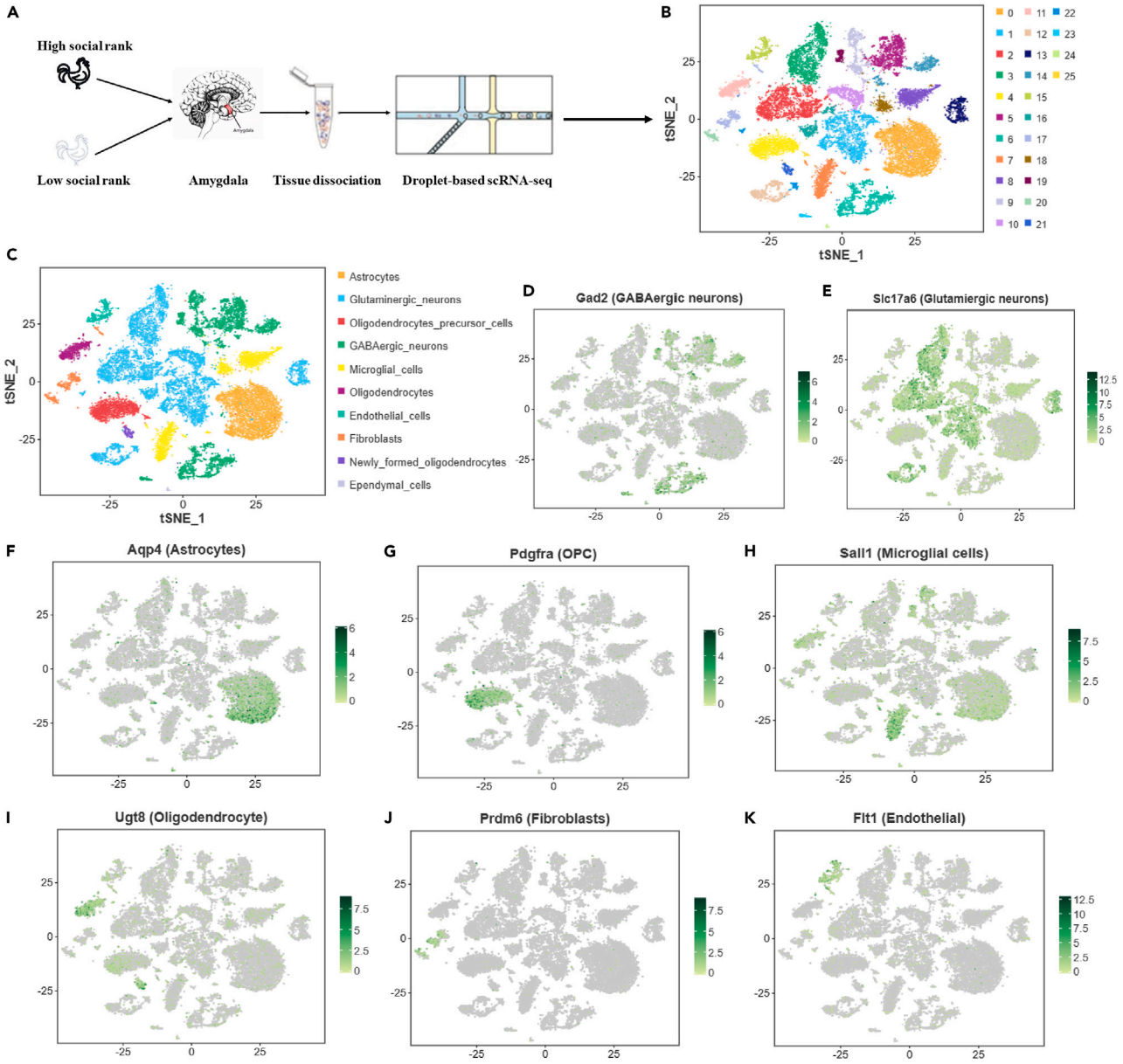

Figure 2. Identification of 26 cell types in chicken amygdala by scRNA-seq

(A) Schematic showing the process of snRNA-seq. After the social hierarchy is established, the amygdala tissue of high and low social hierarchy animals was taken, the frozen amygdala tissue was homogenized, and the 10x Genomics Chromium Controller Instrument was used to generate the scRNA-seq library.

(B) tSNE plot showing the 26 subtypes identified in amygdala. Different colors represent different cell subtypes.

(C) t-SNE plot showing the different cell types in the amygdala based on transcriptome data.

(D–K) Expression of marker genes (highlighted with green color) in the cell types on the t-SNE plot.

Oligodendrocyte differentiation correlates with dynamic transcriptional changes

Cell clusters at different stages provided insights into the transcriptional process of oligodendrocyte differentiation. We made an unsupervised pseudo time analysis by PAGA, where OPC, NFO, and oligodendrocytes were connected on the basis of their gene expression profiles (Figure 5A). Based on the known differentiation direction, we determined OPC as the starting point of differentiation, and the differentiation path was from OPC to NFO to oligodendrocytes (Figure 5A). The gene expression of *pdgfra*, *fyn*, and *cnp* matched this direction (Figure 5C), considering that the pseudo time axis simulated the differentiation process of oligodendrocyte. Analysis of transcriptome data showed that different cell clusters expressed specific gene during cell differentiation. For example, *pdgfra* and *cntfr* were highly expressed in OPC, NFO specifically expressed *arsj* and *lims2*, and oligodendrocytes expressed *st18* and *cdh19* (Figure 5B). Notably, genes (*lims2, znf516, arsj* and so

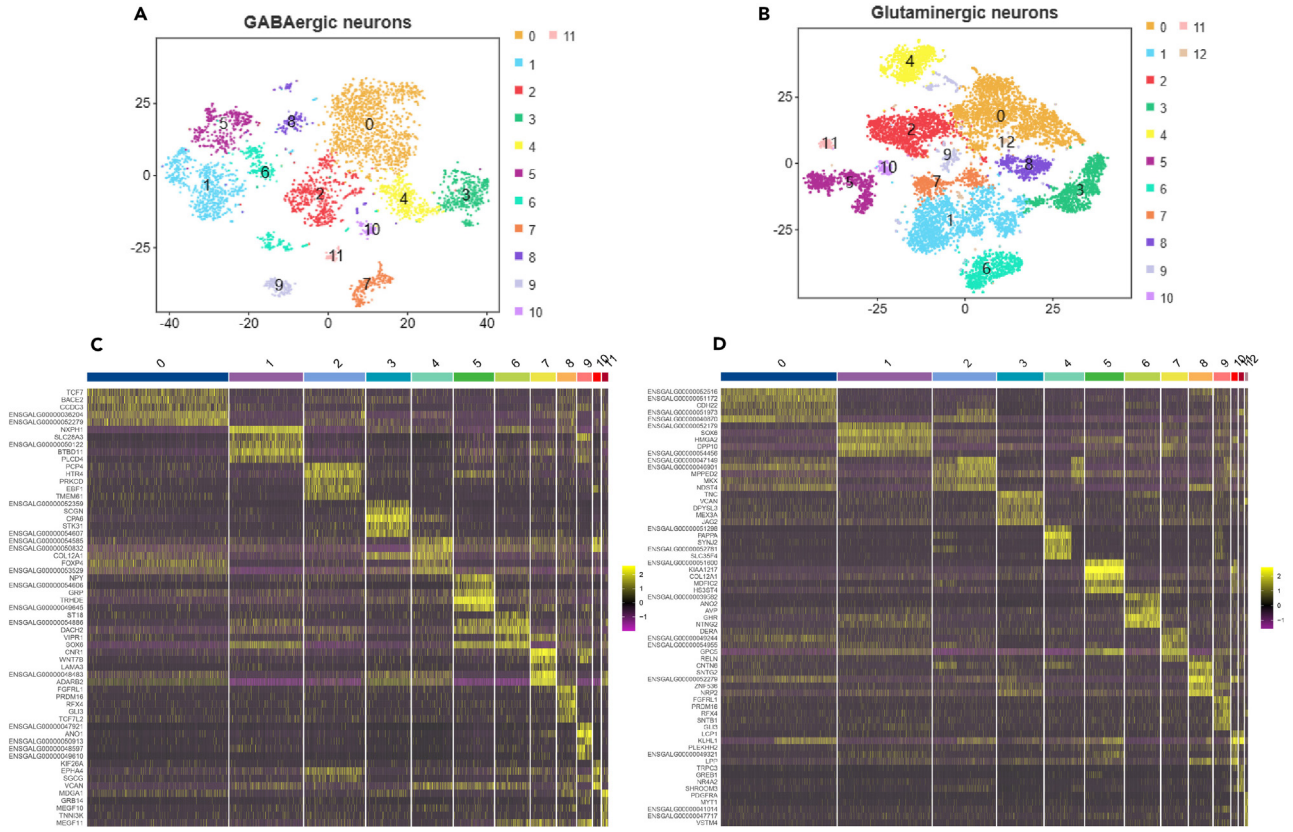

Figure 3. Molecular taxonomy of GABAergic neurons and glutaminergic neurons in the amygdala

(A) Visualization of 12 sub-clusters of GABAergic neurons using two-dimensional tSNE. Different colors represent different cell subtypes.

(B) Visualization of 13 sub-clusters of glutaminergic neurons using two-dimensional tSNE. Different colors represent different cell subtypes.

(C) Heatmap showing the distribution and expression level of significantly differentially expression genes for each sub-cluster of GABAergic neurons. The top 5 variation genes in each sub-cluster are listed on the left.

(D) Heatmap showing the distribution and expression level of significantly differentially expression genes for each sub-cluster of glutaminergic neurons. The top 5 variation genes in each sub-cluster are listed on the left.

on) with high expression in NFO may be important for the transformation from OPC to oligodendrocytes. Gene ontology (GO) analysis showed that the NFO were mainly enriched in biological processes (Figure 5D), while OPC was enriched in biological processes and cellular component for the top 20 GO terms (Figure 4E).These findings indicated that up-regulated gene groups were enriched in different transcripts during different differentiation stages of cell.

Cell type specific transcriptional response to social hierarchy by scRNA-seq

We compared the single cell gene expression profiles between HSR and LSR to check the transcriptional response of amygdala neuron subtypes to different social hierarchy. The results indicated that high and low social hierarchy chickens have different effects on gene expression of neuron subtypes in amygdala, among them, the percentage of GABAergic neurons of HSR (23.07%) was higher than that of LSR (14.21%), and the percentage of glutamatergic neurons of LSR (46.94%) was higher than that of HSR (33.80%) (Figure 6A). Then we made an inter group analysis on these two types of neurons. The sub-clusters of neurons showed that differentially expressed genes (DEGs) were mainly enriched in LGE (Figure 6B) and glu.3 (Figure 7A), DEGs identified in different neuronal clusters are enriched for genes of distinct functions, suggesting that these neuronal sub-clusters may be the main cells in response to social hierarchy.

Then, we carried out GO and Kyoto Encyclopedia of Genes and Genomes (KEGG) analysis on the DEGs in glu.3 and GABA_LGE. In GABA_LGE, DEGs were mainly enriched in biological process and cellular component. For biological process, DEGs were involved in cellular process, single-organism process, biological regulation, metabolic process, response to stimulus, etc (Figure 6C). The main enrichment pathways were energy metabolism, carbohydrate metabolism, nervous system immune system, etc (Figure 6D). In glu.3, for biological process, those DEGs were mainly enriched in cellular process, single-organism process, biological regulation, metabolic process, response to stimulus, etc (Figure 7B). For molecular function, the DGEs were principally involved in binding, catalytic activity, molecular function regulator, transporter activity, etc (Figure 7B). For cellular component, DEGs were significantly enriched in cell, cell part, organelle and etcs (Figure 7B).

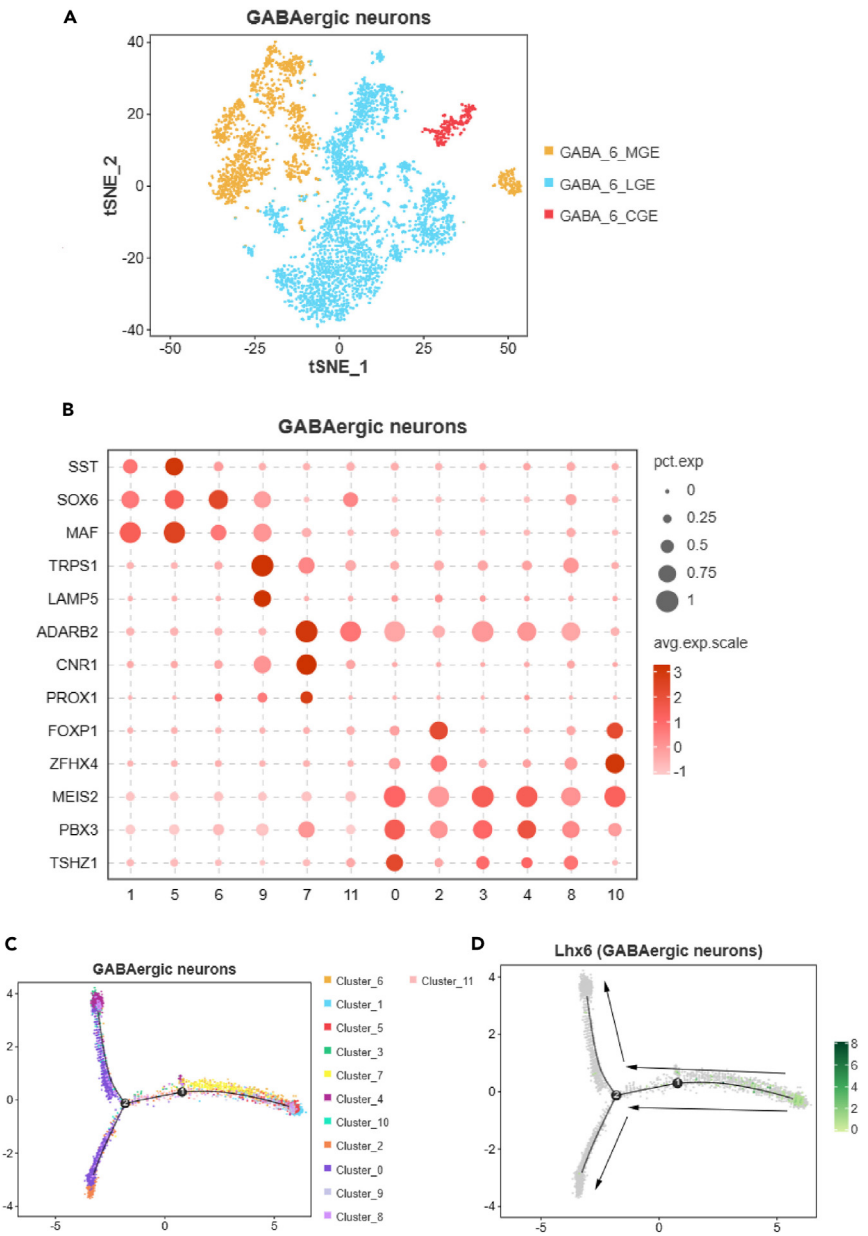

Figure 4. Molecular taxonomy of GABAergic neurons in chicken amygdala

(A) The t-SNE map showed that GABAergic neurons in the amygdala could be further divided into 3 clusters, MGE,LGE,CGE, respectively.

(B) Bubble plots showing the expression of cell type-specific gene markers in different cell clusters.

(C) Pseudo-temporal trajectory maps of 12 subclusters of GABAergic neurons.

(D) Pseudo time showing the possible trajectory of GABAergic neurons depended on biomarkers.

KEGG analysis suggested that the genes were mainly involved in glycan biosynthesis and metabolism, lipid metabolism, endocrine system, nervous system, immune system, translation, folding, sorting and degradation, transport and catabolism, signal transduction and so on (Figure 7C).

Network of potential different gene-gene interactions in response to social hierarchy

In order to explore how glutamatergic and GABAergic neurons regulate the social hierarchy, we identified DEGs through STRING databases and constructed a possible interaction network. In the GABAergic neurons, MCODE plug-in was used to analyze modules in Cytoscape. Modules 1 included 24 nodes and 448 edges with a score of 19.478 (Figure 8A). Modules 2 consisted of 33 nodes and 406 edges with a score of

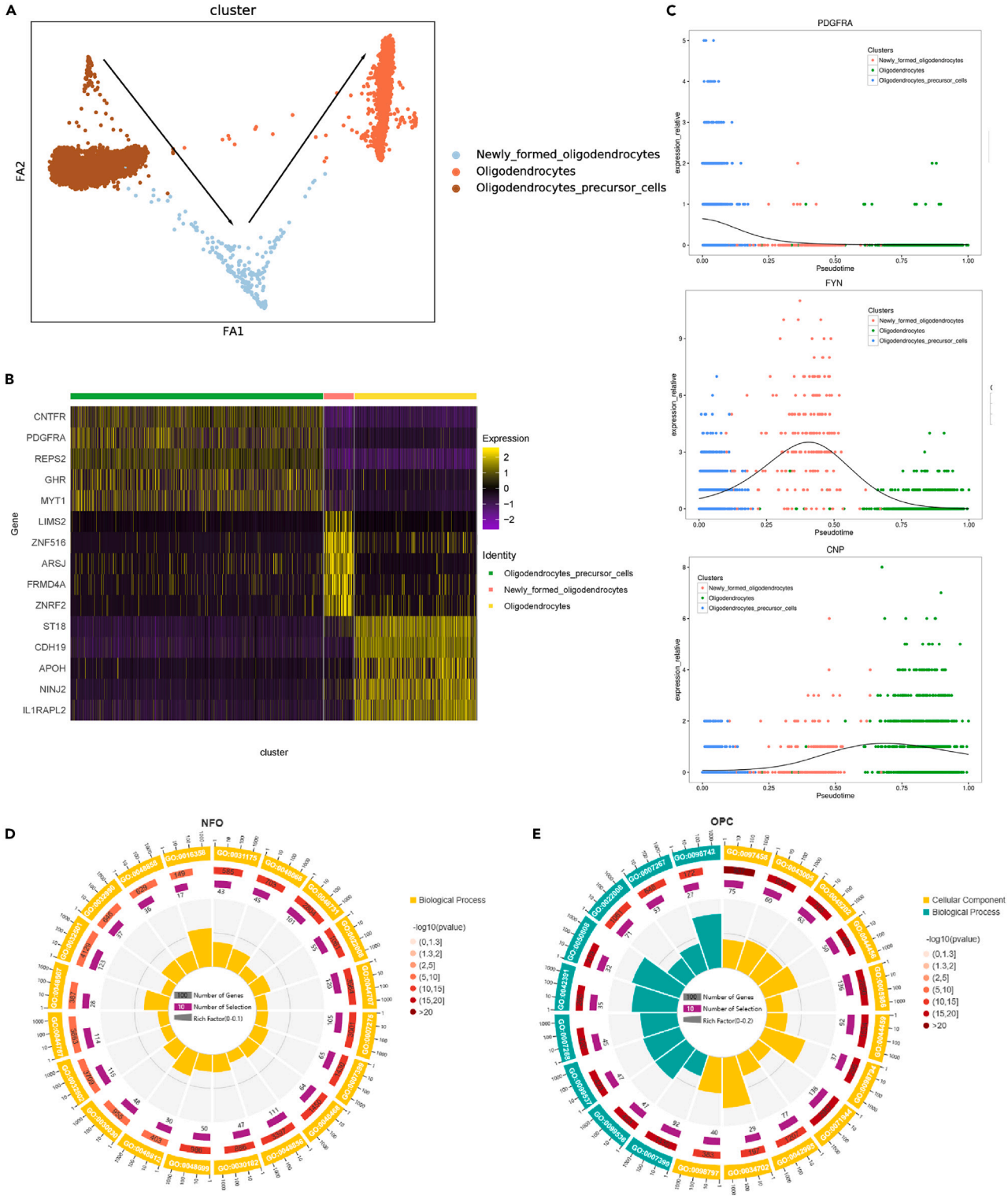

Figure 5. Transcriptional Dynamics during Oligodendrocyte Maturation in chicken amygdala

(A) Unsupervised ordering of oligodendrocytes precursor cells (red), newly formed oligodendrocytes (blue), and oligodendrocytes (dark red) based on their gene expression profiles. Arrows indicate the direction of differentiation.

(B) Heatmap showing the distribution and expression level of significantly differentially expressed top 5 genes for each subcluster.

Figure 5. *Continued*

(C) Scatterplots showing the transcriptional dynamics of pdgfra, fyn, and cnp along the pseudotime. X axis represents the pseudotime axis, y axis shows gene expression level on log scale. Blue, pink, and green dots represent oligodendrocytes precursor cells, newly formed oligodendrocytes, and oligodendrocytes, respectively.

(D) Enrichment circle diagram represents GO analysis results of newly formed oligodendrocytes.

(E) Enrichment circle diagram represents GO analysis results of oligodendrocytes precursor cells.

12.688 (Figure 8B). *RPS6KA2* (ribosomal protein S6 kinase A2), *YWHAH* (3-monooxygenase/tryptophan 5-monooxygenase activation protein eta), *ACTB* (actin, beta), *CDK14* (cyclin dependent kinase 14), *RHOB* (ras homolog family member B) and *PPP2CA* (protein phosphatase 2 catalytic subunit alpha) were selected as hub genes, as these genes were ranked in the top 20 in term of the calculation by five algorithms using five methods in Cytoscape (Table S3). Particularly, most of the top 20 genes were in Module 1, which was more significant in all modules implying that those six genes may play an important role in social hierarchy. Functional and pathway enrichment analysis of this module were conducted using Clue-GO in Cytoscape. GO terms enrichment analysis indicated that genes were mainly enriched in response to hydrogen peroxide, cellular response to carbohydrate stimulus, cyclic-nucleotide phosphodiesterase activity and regulation of cell division (Figure 8E).

In the glutamatergic neurons, we obtained two important modules from the network using MCODE. Modules 1 included 46 nodes and 1696 edges with a score of 37.689 (Figure 8C). Modules 2 included 50 nodes and 1152 edges with a score of 23.510 (Figure 8D). The hub genes were selected as mentioned above (Table S4). These genes were *AKT1* (AKT serine/threonine kinase 1), *SGK1* (serum/glucocorticoid regulated kinase 1), *RHOBTB1* (Rho related BTB domain containing 1), *YES1* (YES proto-oncogene 1, Src family tyrosine kinase), *PKN2* (protein kinase N2), *CDK14* (cyclin dependent kinase 14), *RHOB* (ras homolog family member B), *LRRK1* (leucine rich repeat kinase 1), and *FLT4* (related tyrosine kinase 4). We found that those genes were in module1. Afterward, we conducted functional enrichment analysis on genes in module 1. GO analysis revealed that the pathway of positive regulation of stress-activated MAPK cascade. Besides, cellular response to reactive oxygen species, regulation of epithelial cell migration, phosphatidylinositol phosphate kinase activity, autophagosome assembly and peptidyl-serine phosphorylation pathways were mainly enriched (Figure 8F).

In particular, there are common hub genes *RHOB* and *CDK14* in both the glutamatergic and GABAergic neurons. This implied that these two genes may play an important role in regulating social hierarchy. Afterward, some hub gens were selected for qPCR. The relative fold-change of these selected genes was consistent with scRNA-seq results, suggesting that the transcript identification and abundance estimation were highly reliable (Figure S4).

Comparison of chicken and mammalian amygdala cell clusters

To investigate the conservation and heterogeneity of cell types between species, we integrated data from the amygdala of domestic chickens with published single-cell datasets from the amygdala of human and rhesus monkeys, constructed homologous gene pairs, and submitted the entire population for downscaling clustering, visualization, and other analyses.

Three species were clustered into 37 cell groups annotated into nine cell types, all of which contained cells from all species (Figures 9A and 9B). Each cell type can be identified with high confidence by the expression pf marker genes (Figures 9C–9K) and the results of cell annotation when the reference chickens were analyzed individually (Figure 10A). The nine cell types were GABAergic neurons, glutaminergic neurons, astrocytes, oligodendrocytes, OPC, ependymal cells, endothelial cells, microglial cells, and fibroblasts. To explore the conserved phenotypes of the cell types in the three species, a dendrogram was constructed based on the similarity matrix of cell types in all species (Figure 10B). The most differentiated were the ependymal cells and astrocytes of human with other cell types. The second separated the oligodendrocytes of chicken, human, and rhesus monkeys from other neurons, while the third separated OPC of human from other neurons. Then the OPC, glutaminergic neurons, and GABAergic neurons were on the same branch in chickens, glutaminergic neurons in humans and rhesus monkeys on the same branch, and GABAergic neurons in humans and rhesus monkeys on the same branch. The ependymal cells, astrocytes, fibroblasts, microglial cells, and endothelial cells of chickens were on the same branch; the astrocytes, ependymal cells, fibroblasts, endothelial cells, OPC, and microglial cells of the rhesus monkey were on the same branch; most cell types in humans are not in the same branch as those in chickens and rhesus monkeys. However, three cell types were conserved during evolution in humans and rhesus monkeys, namely oligodendrocytes, glutaminergic neurons and GABAergic neurons, and all cell types were not conserved in humans and rhesus monkeys versus chickens, suggesting that the mammalian cell types were more closely related. When all cell types were combined and compared by species, human and rhesus monkey amygdala cell types were more similar in transcriptome than they were to chicken (Figure 10C).

DISCUSSION

To our knowledge, it is the first study to reveal a cell atlas of chicken amygdala, which provides a foundation for anatomical, physiological, and evolutionary analysis of how amygdala evolves to serve the very different avian amygdala neuron system. Accordingly, we analyzed more than 14,500 single cell transcriptome and identified 25 different cell subtypes in the chicken amygdala. The chicken cell types could be compared to types previously identified in similar studies of human and primate amygdala. Comparing the relationships among amygdala cells in chickens, humans, and primates revealed strong similarities in the overall cell classes. We find that some of the cell types identified in this study are similar to those in the amygdala of rhesus monkeys[21] and mice.[25] However, the results also showed great differences among species in the specific types within each class and the genes that were switched on within each cell type. In the present study, the cell types of human and rhesus monkeys were more closely related and that of chickens were more distant from them. In agreement with the study regarding

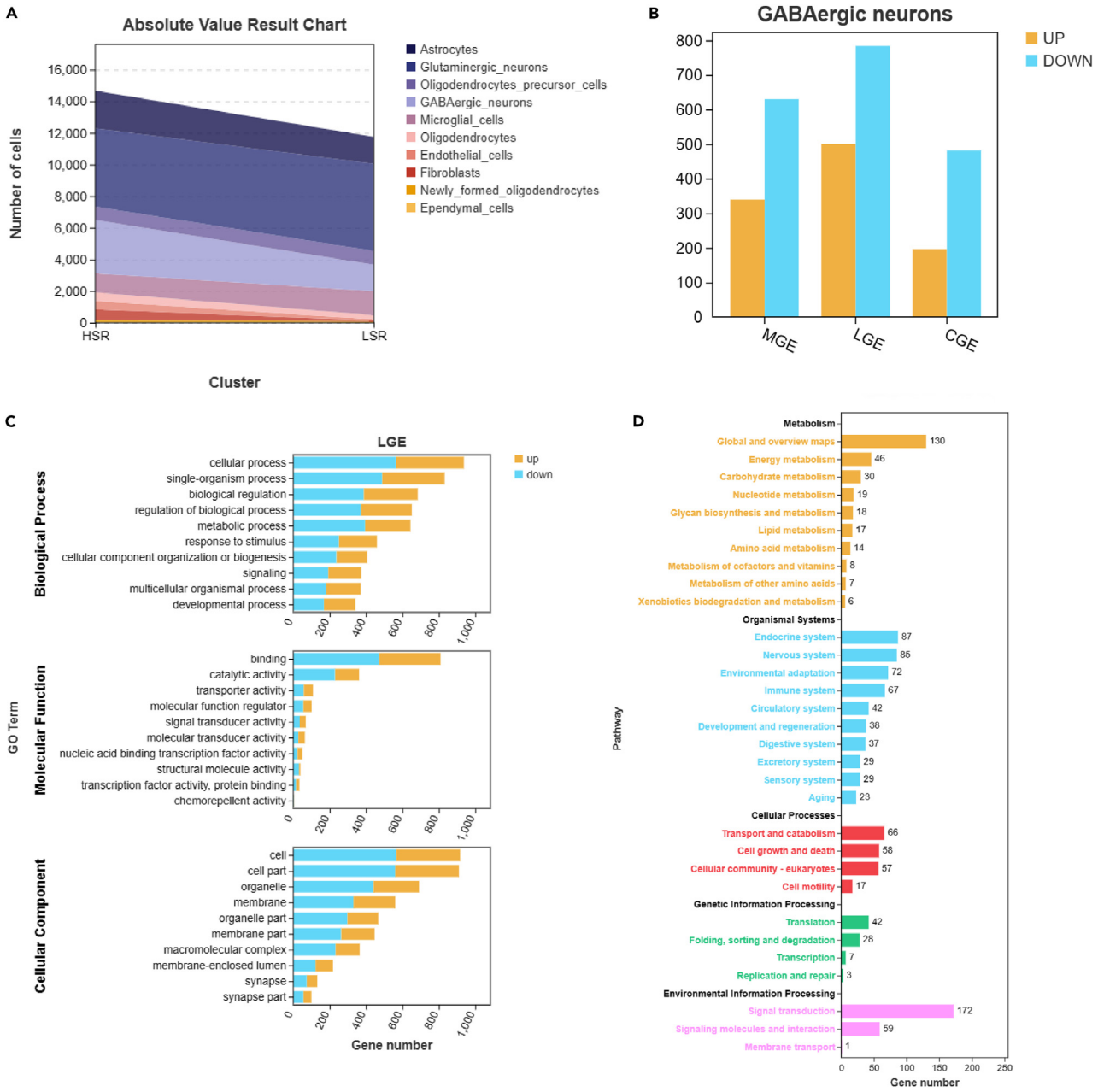

Figure 6. Functional analysis of GABAergic neurons

(A) Graph of absolute value results for each cell type.

(B) The number of up- and downregulated genes in medial ganglionic eminence (MGE), caudal ganglionic eminence (CGE), and lateral ganglionic eminence (LGE).

(C) Results of GO enrichment analysis of LGE.

(D) Results of KEGG enrichment analysis of LGE.

retinal cell types in poultry, human and rhesus monkey cell types were on the same branch, while chicken was not on the same branch as them.[14] Human cell types were not clustered on the same branch, but interspersed between chicken and rhesus monkeys, suggesting that during the evolutionary process, human cell types became more complex as a result of adaptation to the environment. Specifically, for each cell type, oligodendrocytes, glutaminergic neurons, and GABAergic neurons are more closely related in human and rhesus monkeys, and the chicken cell type is not on the same evolutionary branch as either rhesus monkey or human, further demonstrating the specificity of chicken cell types from other species. In the current study, *slc32a1* as a widely accepted marker for GABAergic neurons in vertebrates and

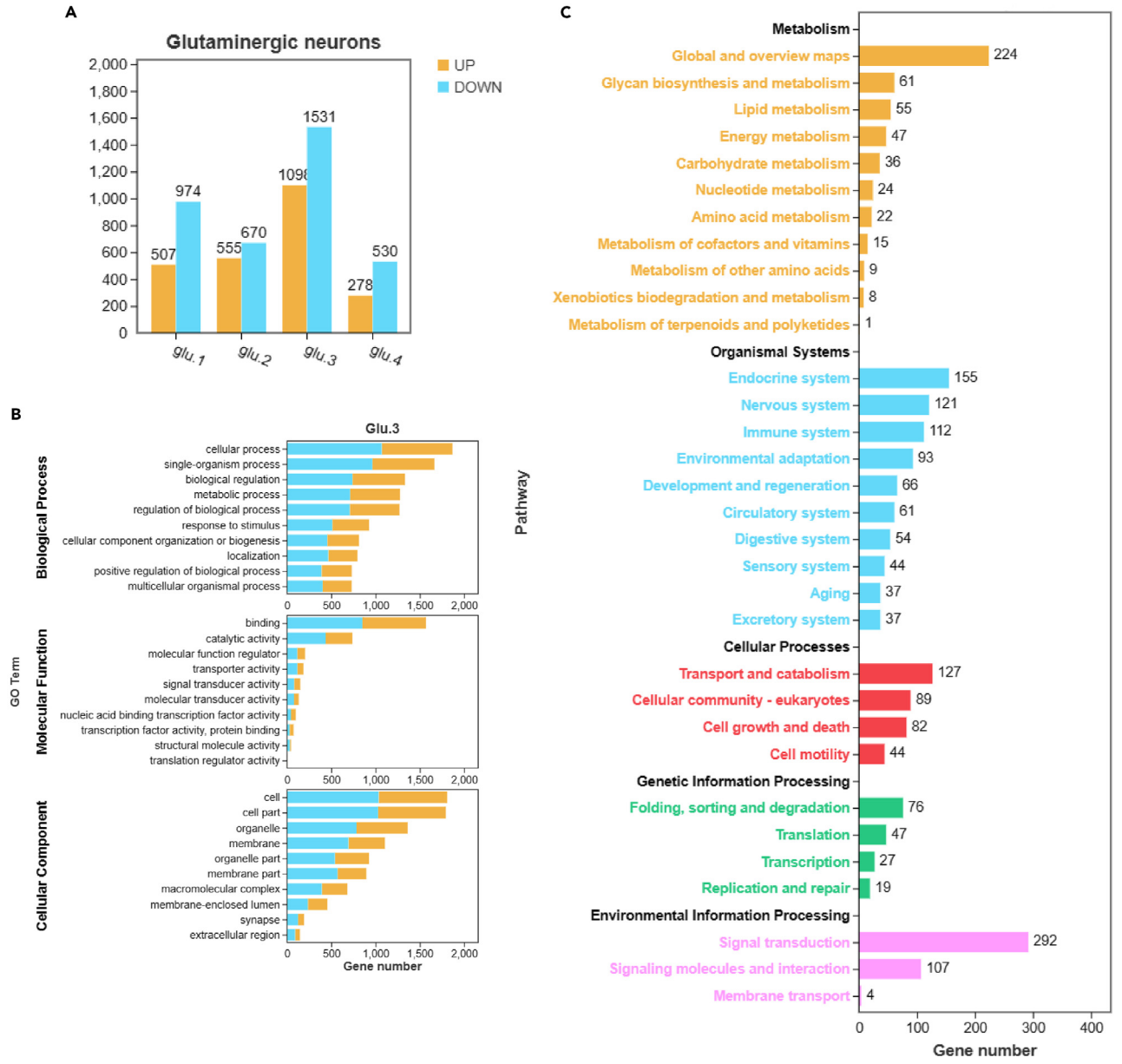

Figure 7. Functional analysis of glutaminergic neurons

(A) The number of up- and down-regulated genes in glu.1, glu.2, glu.3, and glu.4.

(B) Results of GO enrichment analysis of glu.3.

(C) Results of KEGG enrichment analysis of glu.3.

mammals,[26] is also useful to identify for all 12 neuronal sub-clusters of GABAergic neurons in the chicken amygdala. However, serving as central marker genes for glutamatergic neuron in vertebrates and mammals,[21] only *slc17a6* (*vglut2*) but not *slc17a7* (*vglut1*) is detected, suggesting the cell type specific of chicken amygdala from other species. We also find that most non-neuron cells in the amygdala are similar to those in the hypothalamus,[12] hippocampus,[20] and cerebral cortex[20] of mice, which indicates that most non-neuron cells exist in various regions of the brain.

In particular, oligodendrocytes are an important class of glial cells that participate in the formation of the myelin sheath. Myelin formation and regeneration defects will cause transmission disorder and functional loss, leading to cognitive, behavioral, and motor dysfunction.[27] We identify OPC, NFO, and oligodendrocytes and determine the direction of differentiation, indicating that oligodendrocytes differentiation is still taking place in adult chickens. We capture the differentiation process from OPC to oligodendrocytes by the PAGA method, but obtain a different result when it was determined by monocle in mice.[12] We are not clear if the difference is due to species specificity or the algorithm

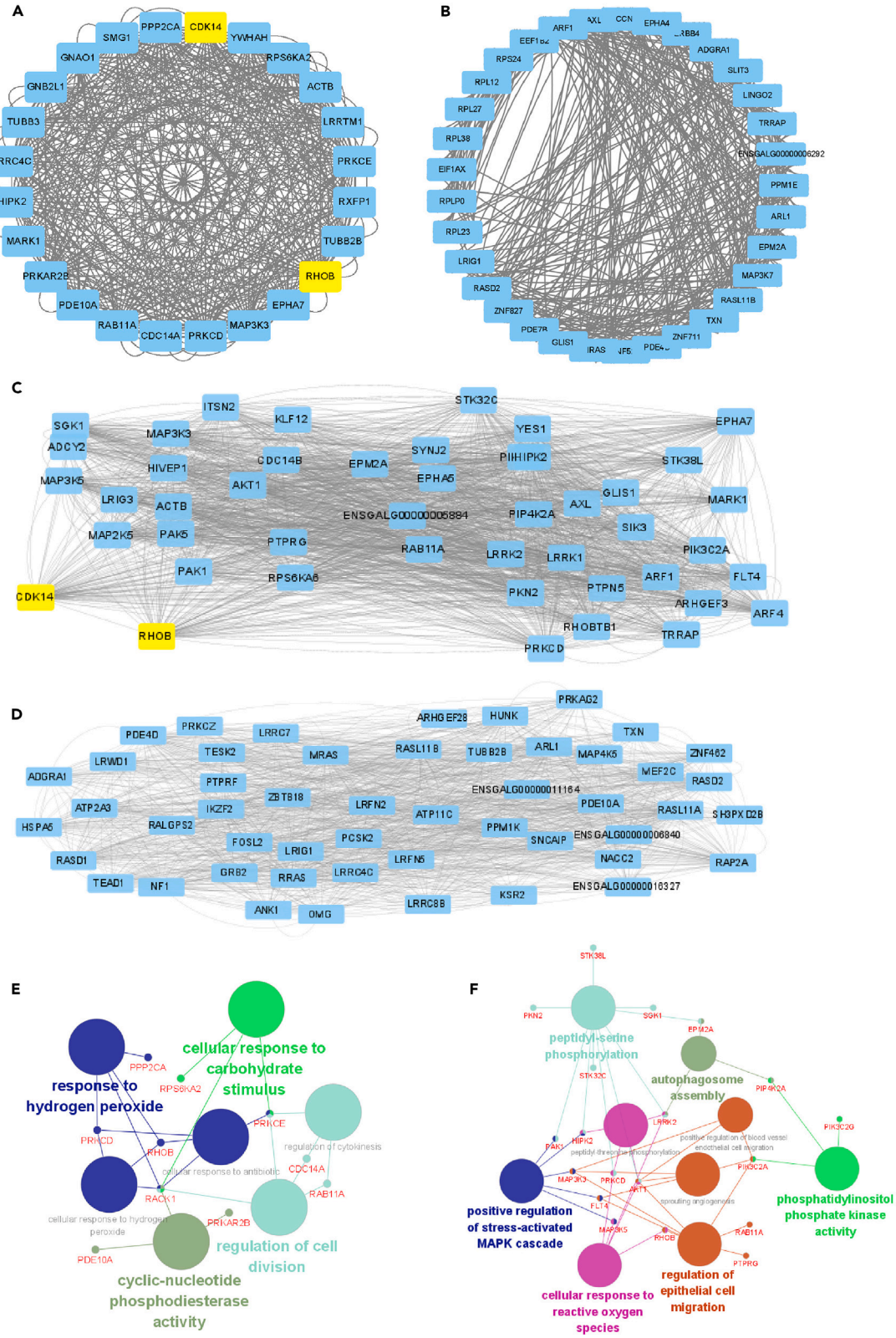
A
SMG1
PPP2CA
CDK14
YWHAH
GNAO1
RPS6KA2
GNB2L1
ACTB
TUBB3
LRRTM1
LRRC4C
PRKCE
HIPK2
RXFP1
MARK1
TUBB2B
PRKAR2B
RHOB
PDE10A
EPHA7
RAB11A
CDC14A
PRKCD
MAP3K3
B
ARF1
EPHA4
ADGRA1
RPS24
SLIT3
RPL12
LINGO2
RPL27
TRRAP
RPL38
ENSGALG00000006292
EIF1AX
PPM1E
RPLP0
ARL1
RPL23
EPM2A
LRIG1
MAP3K7
RASD2
RASL11B
ZNF827
TXN
PDE7B
GLIS1
ZNF711
C
ITSN2
STK32C
SGK1
KLF12
EPHA7
MAP3K3
YES1
ADCY2
SYNJ2
CDC14B
EPM2A
PIIHIPK2
STK38L
HIVEP1
EPHA5
MAP3K5
AKT1
GLIS1
LRIG3
ACTB
ENSGALG00000005884
PIP4K2A
AXL
MARK1
MAP2K5
PAK5
SIK3
PTPRG
RAB11A
LRRK2
LRRK1
PIK3C2A
PAK1
RPS6KA6
ARF1
FLT4
CDK14
PKN2
PTPN5
ARHGEF3
ARF4
RHOB
RHOBTB1
TRRAP
PRKCD
D
PRKAG2
ARHGEF28
HUNK
PRKCZ
PDE4D
LRRC7
TXN
TESK2
MRAS
RASL11B
TUBB2B
ARL1
MAP4K5
ZNF462
LRWD1
MEF2C
ADGRA1
PTPRF
RASD2
ENSGALG00000011164
ZBTB18
ATP2A3
IKZF2
LRFN2
ATP11C
PDE10A
RASL11A
SH3PXD2B
HSPA5
RALGPS2
PPM1K
SNCAIP
ENSGALG00000006840
FOSL2
PCSK2
LRIG1
NACC2
RAP2A
RASD1
LRFN5
GRB2
RRAS
LRRC4C
TEAD1
NF1
ENSGALG00000016327
KSR2
ANK1
OMG
LRRC8B
E
cellular response to carbohydrate stimulus
response to hydrogen peroxide
PPP2CA
RPS6KA2
PRKCE
PRKCD
RHOB
regulation of cytokinesis
cellular response to antibiotic
CDC14A
RAB11A
RACK1
cellular response to hydrogen peroxide
PRKAR2B
PDE10A
regulation of cell division
cyclic-nucleotide phosphodiesterase activity
F
STK38L
PKN2
SGK1
peptidyl-serine phosphorylation
EPM2A
STK32C
autophagosome assembly
PIP4K2A
LRRK2
PIK3C2G
positive regulation of blood vessel endothelial cell migration
PAK1
HIPK2
peptidyl-threonine phosphorylation
PIK3C2A
MAP3K3
PRKCD
AKT1
sprouting angiogenesis
phosphatidylinositol phosphate kinase activity
positive regulation of stress-activated MAPK cascade
FLT4
MAP3K5
RHOB
RAB11A
PTPRG
regulation of epithelial cell migration
cellular response to reactive oxygen species

Figure 8. PPI network construction and analyses

(A) PPI network of module 1 in GABAergic neurons.

(B) PPI network of module 2 in GABAergic neurons.

(C) PPI network of module 1 in glutaminergic neurons.

(D) PPI network of module 2 in glutaminergic neurons.

(E) Functions and pathways of the module 1 were computed and visualized using ClueGO in GABAergic neurons.

(F) Functions and pathways of the module 1 were computed and visualized using ClueGO in glutaminergic neurons.

itself. Importantly, the developmental trajectory in our study is similar to that in other studies,[12] which further validates our analytical method. Regardless of oligodendrocytes known to cause behavioral dysfunction, their association with social behavior is rare reported. We thus did not conduct further analysis, but these results did contribute to a catalog of cell atlas for chicken amygdala worthy of further studies to understand the avian brain and neuron types. As is known, dopamine and serotonin system are important neurotransmitters in the brain, controlling behavior, cognition, memory, and reward.[28] The two systems are well demonstrated to be related with aggressive interactions and social behaviors.[29] However, both the dopamine and serotonin neurons in chicken amygdala were not identified by marker genes that were already reported in the brain of mice and human.[28,30] These findings did again prove the cell type specific among species, which provide new insights to the cell atlas of chicken amygdala. As a result, we focus on the GABAergic and glutamatergic neurons, which are also known to be related to social behaviors.[31] GABAergic and glutamatergic neurons are the main neurons in the amygdala,[1] which are connected to form a network to perform various functions, such as mediating aggression, fear behavior and memory.[32] During brain development, most interneurons originate from ganglia protrusions (GEs), which can be divided into LGE, MGE, and CGE.[33] In our study, we also further divide GABA neurons into LGE, MGE, and CGE, referring to the reported marker genes.[22,34] MGE-class neuron significantly expresses SST cortical interneurons, which is consistent with human research that SST cortical interneurons derive primarily from the MGE-class neuron.[34] Worth notably, SST cortical interneurons are associated with circuit plasticity during reward tasks and motor learning in mice.[35] We determined the starting point of differentiation according to GABAergic progenitor cells, indicating that GABA neurons have a differentiation relationship in the chicken amygdala. Glutamate neurons are the main excitatory neurons in the amygdala, which is associated with learning and memory function, promoting self-grooming and inhibiting social interaction in mice.[36] Glutamatergic neurons, containing many subtypes cell, are more complex than GABA neurons. Accordingly, the subtypes cell of glutamate neurons were divided in light of the layer and projection pattern[37] and the co-expressed genes.[26] In this study, we obtain four different glutamatergic neurons subgroups, called glu.1, glu.2, glu.3, and glu.4. However, the branch results by pseudotime analysis are inconsistent with the four subgroups. Furthermore, we could not determine the starting point and direction of differentiation of glutamate neurons according to the marker gene reported in mice.[38] These results again provide evidences to the cell-specific of amygdala among avian, vertebrate and mammals. Increased evidences show that social hierarchy affects transcriptomic patterns of animals. In mice, dominant animals mainly participate in the specific gene expression related to urine production and catabolism, while subdominant animals show higher gene expression that related to the promotion of the biosynthesis process, wound healing and inflammatory response,[39] and oxidative phosphorylation and DNA repair.[39] In this study, the GO terms are mainly focused on cellular process, biological regulation, metabolic process, and response to stimulation. The KEGG pathways are mainly relative to energy metabolism, nervous system and immune system, which is similar with a previous study investigated on the effect of social hierarchy on bees.[40] Interestingly, the transcripts differentially expressed between animals with different social rank are related to GABA and glutamate.[41] In this study, the high rank chickens have more GABA neuron and less glutamate neurons than the low rank chickens, which suggests the essential role of GABA and glutamate neurons on the social hierarchy of chickens. We find that LGE of GABA neuron has the most differential genes. Besides, LGE-class neuron forms a disinhibitory circuit that is strongly regulated by dopamine in the amygdala of mammalian cerebral cortex,[42] which suggests that the LGE cells may play an important role in regulating social hierarchy. Marker genes for cortical interneurons and olfactory bulb interneurons have not been clearly distinguished in poultry. However, of the marker genes, we find MGE-class neuron is similar to the SST cortical interneurons, LGE-class neuron similar to the olfactory bulb interneurons, and CGE-class neuron similar to CGE generated cortical interneurons according to the mammals and songbird studies.[22,34] The increase of GABA neurotransmission in the amygdala will lead to the behavioral changes induced by social stressor, and provide protection in dominant animals when suffer stress.[41] Additionally, the GABAergic neuron is found to promote aggressive behaviors, while glutamatergic neurons promote self-grooming behavior and inhibit social interaction in a mouse amygdala study.[36] Notably, aggression may also be mediated by glutamate neurons, and that is a possibility that the promotion of aggression by GABAergic neurons is via inhibiting glutamatergic neurons.[43] After brain trauma, the expression of Decorin (*dcn*) in the excitatory neurons of the amygdala (glutamatergic neurons) increases significantly. Furthermore, knocking out the *dcn* in the amygdala can alleviate the fear, which is due to the decrease in the *dcn* expression mediated perineural networks (PNNs).[25] That is possible that behaviors are involved with various neurons.

Until now, there are increased studies regarding on the underpinned mechanism of social hierarchy in vertebrate and mammalian. In this study, we find out that the social rank of roosters tends to be stable along as the age, which is consistent with a previous rhesus monkey study. Likewise, the mRNA expression of glucocorticoid receptor, *CRH, GNRH1*, and *BDNF* of amygdala in dominant mice was higher than those in subdominant mice.[44] In this study, we also find some genes that may related to social hierarchy, suh as *AKT1, SGK1, RHOBTB1, YES1, PKN2, CDK14, RHOB, LRRK1*, and *FLT4* in glutamate neurons, and *RPS6KA, YWHAH, ACTB, CDK14, RHOB*, and *PPP2CA* in GABA neuron. Of these, the genes *CDK14* and *RHOB* are candidate genes both in GABAergic and glutamatergic neurons. *RHOB* plays an important role in the process of chicken neural development, which is induced by the transcription factor SOX5 in the chicken head neural crest before migration.[45] Besides, *RHOB* is related to inflammatory reaction.[46] We find that the high-rank chickens have higher expression of *RHOB* than low-rank

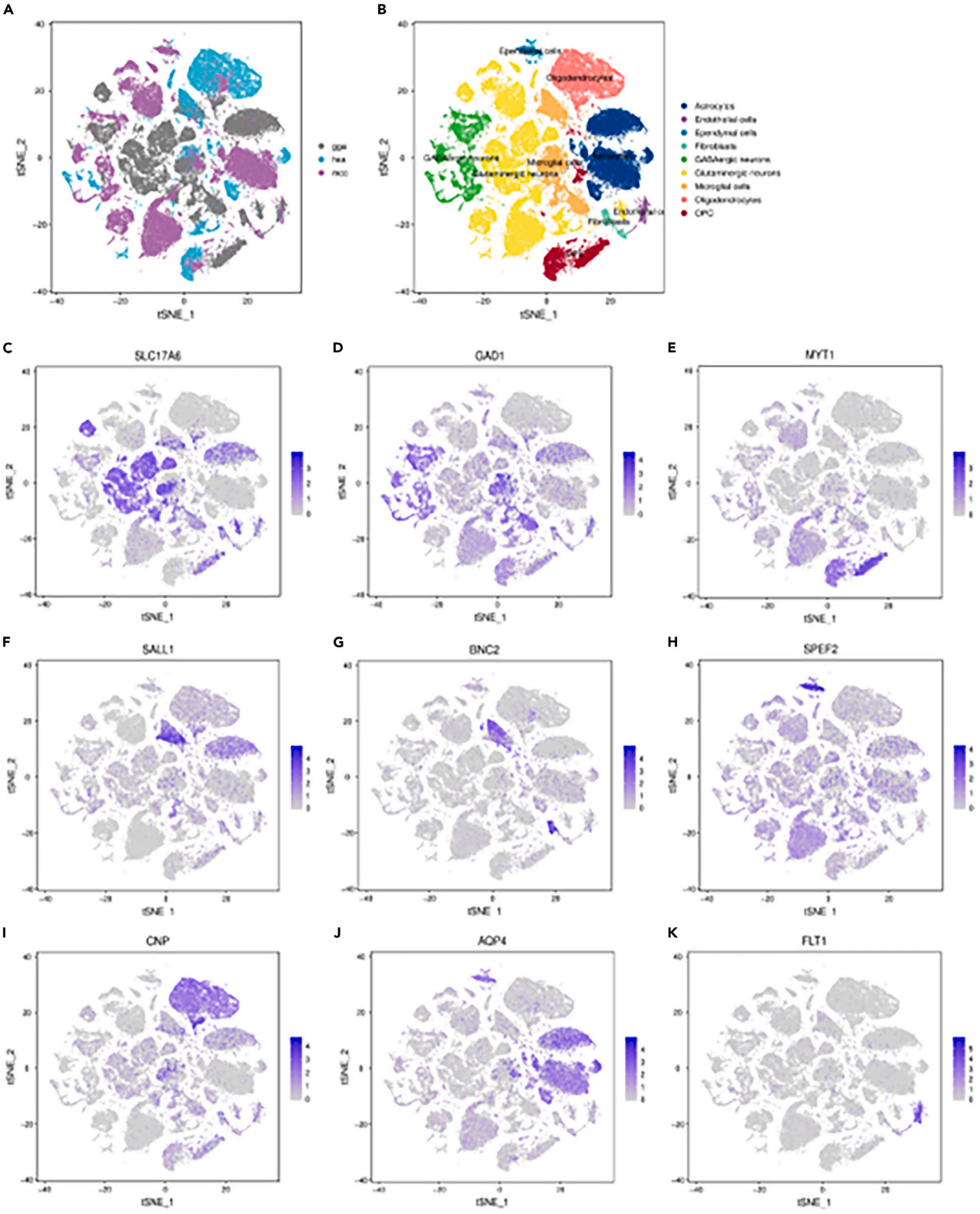
A
B
C
SLC17A6
D
GAD1
E
MYT1
F
SALL1
G
BNC2
H
SPEF2
I
CNP
J
AQP4
K
FLT1
tSNE_1
tSNE_2

Figure 9. t-SNE plot showing the different cell types in the amygdala of chicken, human and rhesus monkey based on transcriptome data

(A) t-SNE visualization of pooled cells from chicken, human, rhesus monkey, following unsupervised clustering. Colors indicate species.

(B) The same as A, but colors distinguish different cell types.

(C–K) Feature plot showing the canonical markers of each retina cell class.

individuals, which may suggest better immune functions in dominant than subdominant animals. This is in line with a previous study indicated that high ranking rhesus macaques have stronger abilities in response to immune challenges.[7] *CDK14*, a Wnt signal molecule, is related to neural plasticity in the amygdala. In mice, the expression of *CDK14* in amygdala is related to fear.[47] In the current study, low-rank chickens show upregulated *CDK14* expression than high-rank chickens. In a stable group, mice with low social hierarchy would avoid conflicts from high social hierarchy individuals by observing and abiding rules, so as to maintain the long-term interests, and is probably associated with fear.[48] The fear is mediated by certain neurons in the amygdala. For example, GABAergic neurons are crucial for the acquisition and expression of rodent conditioned fear and conditioned social failure.[4] When exposed to long-term fear, the cerebrospinal oxytocin concentration in dominant monkeys was higher[49] while the expression of brain-derived neurotrophic factor (*BDNF*) in the amygdala of dominant mice[50] was significantly increased as compared to subdominant animals. Notably, *SGK1* is obviously expressed under stress, while plays a protective role responding to the stressor.[51] Our result of higher *SGK1* expression in individuals with low social rank suggested that low rank individuals are subjected to more stress during the establishment of social rank. However, we did have limitations on the network of potential genes and their possible functions and interactions in response to social hierarchy due to the lack of biological duplication of the amygdala samplings. A comprehensive study should be further conducted to figure out the underpinned mechanism of the interaction of amygdala neurons with social hierarchy in chickens.

Conclusions

In summary, we performed cross-species analysis of mammalian amygdala single-cell atlases with poultry, and found out that cell types of human and rhesus monkeys were more closely related and that of chickens were more distant from them. We identified 26 clusters and divided it into 10 main clusters including GABAergic neurons, glutaminergic neurons, astrocytes, oligodendrocytes, OPCs, newly formed oligodendrocytes ependymal cells, endothelial cells, microglial cells, and fibroblasts. Of which, the GABAergic and glutamatergic neurons are known to be associated with social behaviors, and their sub-neurons of GABA_LEG and Glu3 are considered as main neurons mediating the establishment of social hierarchy in chickens. By the analysis of MCODE plug-in, the common hub genes *RHOB* and *CDK14* are found in both the glutamatergic and GABAergic neurons. Our results provide to serve the developmental studies of the avian amygdala neuron system, and new insights into the underpinned mechanism of social hierarchy in poultry.

Limitations of the study

Several questions remain unanswered in this study: How do GABAergic and glutamatergic neurons regulate the social hierarchy of chickens? Does the genes *RHOB* and *CDK14* play roles in the formation of social hierarchy in roosters? These questions will require further investigations.

STAR★METHODS

Detailed methods are provided in the online version of this paper and include the following:

- KEY RESOURCES TABLE
- RESOURCE AVAILABILITY
  - Lead contact
  - Materials availability
  - Data and code availability
- EXPERIMENTAL MODEL AND STUDY PARTICIPANT DETAILS
  - Method details

SUPPLEMENTAL INFORMATION

Supplemental information can be found online at https://doi.org/10.1016/j.isci.2024.109880.

ACKNOWLEDGMENTS

This study was supported the National Natural Science Foundation of China (32102596), the the major projects in agricultural biology breeding (2023ZD0406401), the Natural Science Foundation of Guangdong Province (2024A151501233), and Guangdong Provincial Key Laboratory of Animal Molecular Design and Precise Breeding (2019B030301010). We thank the farm staff at Guangdong Tinoo's FOODS Group Co., Ltd. (Qingyuan County, Guangdong, China) for their assistance during the project.

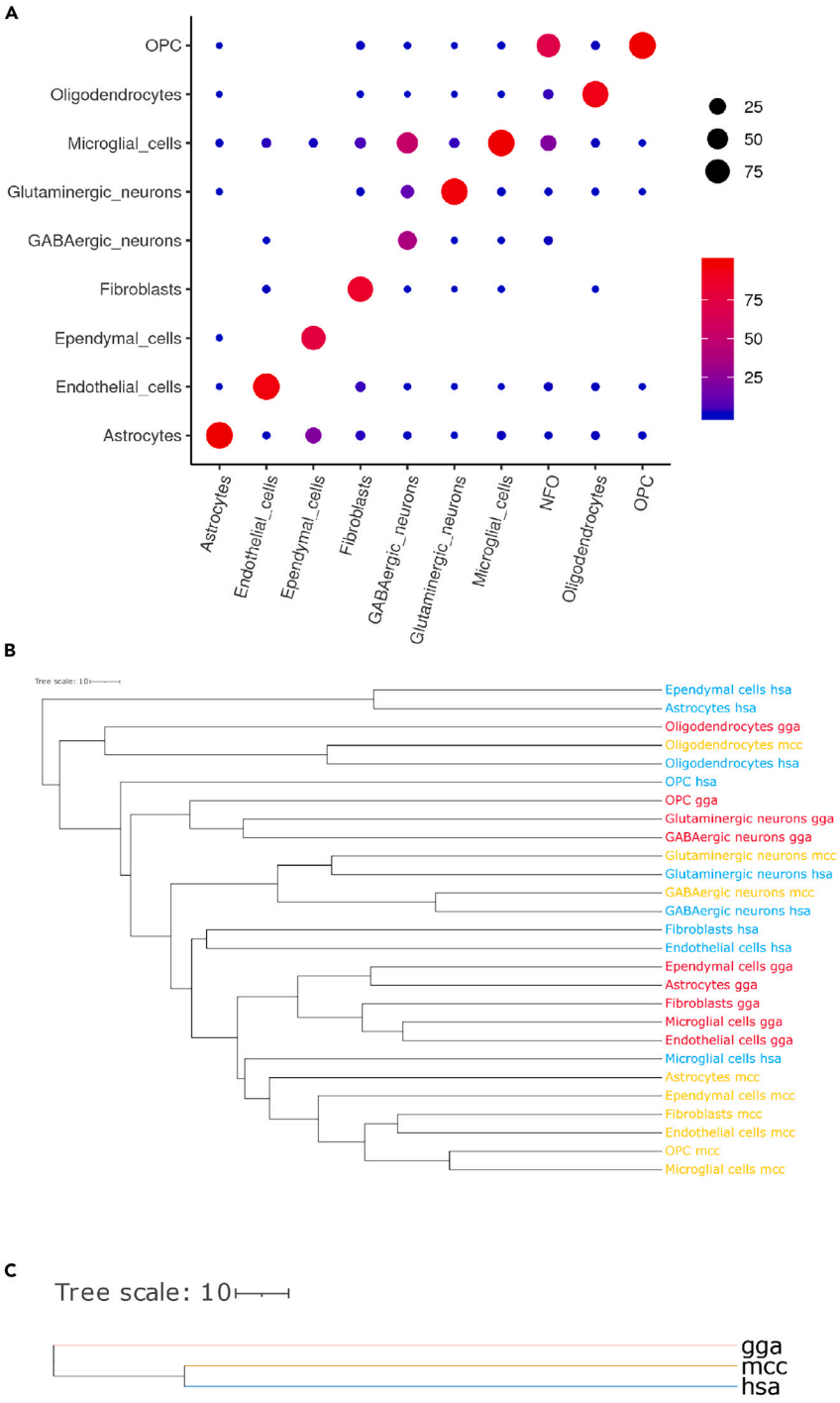

Figure 10. The evolutionary relationship between chickens, humans, and rhesus monkeys

(A) Correlation analysis of cell annotation results between chicken and cross species analysis. The horizontal axis represents the annotation results of the chicken, and the vertical axis represents the annotation results of three species.

(B) Dendrogram based on overall amygdala cell transcriptomic similarity among the three species.

(C) Dendrogram based on the transcriptomic similarity of cell classes from each species.

AUTHOR CONTRIBUTIONS

S.C. and H.L. designed the study, S.C. and L.X. wrote the manuscript. L.X., H.D., and D.Z. conducted experiments, L.X., Z.X., L.Z, M.Z., Z.M., H.Z., and J.L. analyzed experimental results, H.Y. and J.G. guided animal experiments and established the social hierarchy of domestic chickens. All authors contributed to the data interpretation and approved the final version of the manuscript.

DECLARATION OF INTERESTS

The authors declare that they have no conflict of interest.

Received: December 5, 2023
Revised: February 29, 2024
Accepted: April 29, 2024
Published: May 3, 2024

REFERENCES

1. Janak, P.H., and Tye, K.M. (2015). From circuits to behaviour in the amygdala. Nature *517*, 284–292.
2. West, A.E., and Greenberg, M.E. (2011). Neuronal activity–regulated gene transcription in synapse development and cognitive function. Cold Spring Harb. Perspect. Biol. *3*, a005744.
3. Rosvold, H.E., Mirsky, A.F., and Pribram, K.H. (1954). Influence of amygdalectomy on social behavior in monkeys. J. Comp. Physiol. Psychol. *47*, 173–178.
4. Jasnow, A.M., and Huhman, K.L. (2001). Activation of GABAA receptors in the amygdala blocks the acquisition and expression of conditioned defeat in Syrian hamsters. Brain Res. *920*, 142–150.
5. Zhou, T., Zhu, H., Fan, Z., Wang, F., Chen, Y., Liang, H., Yang, Z., Zhang, L., Lin, L., Zhan, Y., et al. (2017). History of winning remodels thalamo-PFC circuit to reinforce social dominance. Science *357*, 162–168.
6. Ma, M., Xiong, W., Hu, F., Deng, M.-F., Huang, X., Chen, J.-G., Man, H.-Y., Lu, Y., Liu, D., and Zhu, L.-Q. (2020). A novel pathway regulates social hierarchy via lncRNA AtLAS and postsynaptic synapsin IIb. Cell Res. *30*, 105–118.
7. Snyder-Mackler, N., Sanz, J., Kohn, J.N., Brinkworth, J.F., Morrow, S., Shaver, A.O., Grenier, J.-C., Pique-Regi, R., Johnson, Z.P., Wilson, M.E., et al. (2016). Social status alters immune regulation and response to infection in macaques. Science *354*, 1041–1045.
8. Wang, Y., Dai, G., Gu, Z., Liu, G., Tang, K., Pan, Y.-H., Chen, Y., Lin, X., Wu, N., Chen, H., et al. (2020). Accelerated evolution of an Lhx2 enhancer shapes mammalian social hierarchies. Cell Res. *30*, 408–420.
9. Gospocic, J., Glastad, K.M., Sheng, L., Shields, E.J., Berger, S.L., and Bonasio, R. (2021). Kr-h1 maintains distinct caste-specific neurotranscriptomes in response to socially regulated hormones. Cell *184*, 5807–5823.e14.
10. Ding, J., Adiconis, X., Simmons, S.K., Kowalczyk, M.S., Hession, C.C., Marjanovic, N.D., Hughes, T.K., Wadsworth, M.H., Burks, T., Nguyen, L.T., et al. (2020). Systematic comparison of single-cell and single-nucleus RNA-sequencing methods. Nat. Biotechnol. *38*, 737–746.
11. Russell, A.B., Trapnell, C., and Bloom, J.D. (2018). Extreme heterogeneity of influenza virus infection in single cells. Elife *7*, e32303.
12. Chen, R., Wu, X., Jiang, L., and Zhang, Y. (2017). Single-cell RNA-seq reveals hypothalamic cell diversity. Cell Rep. *18*, 3227–3241.
13. Hochgerner, H., Tibi, M., Netser, S., Ophir, O., Reinhardt, N., Singh, S., Lin, Z., Wagner, S., and Zeisel, A. (2022). Cell types in the mouse amygdala and their transcriptional response to fear conditioning. Preprint at bioRxiv. https://doi.org/10.1101/2022.10.25.513733.
14. Yamagata, M., Yan, W., and Sanes, J.R. (2021). A cell atlas of the chick retina based on single-cell transcriptomics. Elife *10*, e63907.
15. Feregrino, C., Sacher, F., Parnas, O., and Tschopp, P. (2019). A single-cell transcriptomic atlas of the developing chicken limb. BMC Genom. *20*, 401.
16. Li, J., Xing, S., Zhao, G., Zheng, M., Yang, X., Sun, J., Wen, J., and Liu, R. (2020). Identification of diverse cell populations in skeletal muscles and biomarkers for intramuscular fat of chicken by single-cell RNA sequencing. BMC Genom. *21*, 752.
17. Mantri, M., Scuderi, G.J., Abedini-Nassab, R., Wang, M.F.Z., McKellar, D., Shi, H., Grodner, B., Butcher, J.T., and De Vlaminck, I. (2021). Spatiotemporal single-cell RNA sequencing of developing chicken hearts identifies interplay between cellular differentiation and morphogenesis. Nat. Commun. *12*, 1771.
18. Estermann, M.A., Williams, S., Hirst, C.E., Roly, Z.Y., Serralbo, O., Adhikari, D., Powell, D., Major, A.T., and Smith, C.A. (2020). Insights into gonadal sex differentiation provided by single-cell transcriptomics in the chicken embryo. Cell Rep. *31*, 107491.
19. Rotta, R., and Noack, A. (2011). Multilevel local search algorithms for modularity clustering. ACM J. Exp. Algorithmics *16*, 2.1–2.27.
20. Zeisel, A., Muñoz-Manchado, A.B., Codeluppi, S., Lönnerberg, P., La Manno, G., Juréus, A., Marques, S., Munguba, H., He, L., Betsholtz, C., et al. (2015). Cell types in the mouse cortex and hippocampus revealed by single-cell RNA-seq. Science *347*, 1138–1142.
21. Zhang, L., Cheng, Y., Wu, S., Lu, Y., Xue, Z., Chen, D., Zhang, B., Qiu, Z., and Jiang, H. (2020). The molecular taxonomy of primate amygdala via single-nucleus RNA-sequencing analysis. Preprint at bioRxiv. https://doi.org/10.1101/2020.07.29.226829.
22. Colquitt, B.M., Merullo, D.P., Konopka, G., Roberts, T.F., and Brainard, M.S. (2021). Cellular transcriptomics reveals evolutionary identities of songbird vocal circuits. Science *371*, eabd9704.
23. Mayer, C., Hafemeister, C., Bandler, R.C., Machold, R., Batista Brito, R., Jaglin, X., Allaway, K., Butler, A., Fishell, G., and Satija, R. (2018). Developmental diversification of cortical inhibitory interneurons. Nature *555*, 457–462.
24. Guo, T., Liu, G., Du, H., Wen, Y., Wei, S., Li, Z., Tao, G., Shang, Z., Song, X., Zhang, Z., et al. (2019). Dlx1/2 are central and essential components in the transcriptional code for generating olfactory bulb interneurons. Cereb. Cortex *29*, 4831–4849.
25. Shi, Y., Wu, X., Zhou, J., Cui, W., Wang, J., Hu, Q., Zhang, S., Han, L., Zhou, M., Luo, J., et al. (2022). Single-Nucleus RNA Sequencing Reveals that Decorin Expression in the Amygdala Regulates Perineuronal Nets Expression and Fear Conditioning Response after Traumatic Brain Injury. Adv. Sci. *9*, 2104112.
26. Mickelsen, L.E., Bolisetty, M., Chimileski, B.R., Fujita, A., Beltrami, E.J., Costanzo, J.T., Naparstek, J.R., Robson, P., and Jackson, A.C. (2019). Single-cell transcriptomic analysis of the lateral hypothalamic area reveals molecularly distinct populations of inhibitory and excitatory neurons. Nat. Neurosci. *22*, 642–656.
27. Franklin, R.J.M., and Goldman, S.A. (2015). Glia disease and repair—remyelination. Cold Spring Harb. Perspect. Biol. *7*, a020594.
28. Tiklová, K., Björklund, Å.K., Lahti, L., Fiorenzano, A., Nolbrant, S., Gillberg, L., Volakakis, N., Yokota, C., Hilscher, M.M., and Hauling, T. (2019). Single-cell RNA sequencing reveals midbrain dopamine neuron diversity emerging during mouse brain development. Nat. Commun. *10*, 1–12.
29. Qu, C., Ligneul, R., Van der Henst, J.-B., and Dreher, J.-C. (2017). An integrative interdisciplinary perspective on social dominance hierarchies. Trends Cogn. Sci. *21*, 893–908.
30. Smits, L.M., Magni, S., Kinugawa, K., Grzyb, K., Luginbühl, J., Sabate-Soler, S., Bolognin, S., Shin, J.W., Mori, E., Skupin, A., and Schwamborn, J.C. (2020). Single-cell transcriptomics reveals multiple neuronal cell types in human midbrain-specific organoids. Cell Tissue Res. *382*, 463–476.
31. Chen, P., and Hong, W. (2018). Neural circuit mechanisms of social behavior. Neuron *98*, 16–30.
32. Hermans, E.J., Battaglia, F.P., Atsak, P., de Voogd, L.D., Fernández, G., and Roozendaal, B. (2014). How the amygdala affects emotional memory by altering brain network properties. Neurobiol. Learn. Mem. *112*, 2–16.
33. Zhao, Z., Zhang, D., Yang, F., Xu, M., Zhao, S., Pan, T., Liu, C., Liu, Y., Wu, Q., Tu, Q., et al. (2022). Evolutionarily conservative and

non-conservative regulatory networks during primate interneuron development revealed by single-cell RNA and ATAC sequencing. Cell Res. *32*, 425–436.
34. Delgado, R.N., Allen, D.E., Keefe, M.G., Mancia Leon, W.R., Ziffra, R.S., Crouch, E.E., Alvarez-Buylla, A., and Nowakowski, T.J. (2022). Individual human cortical progenitors can produce excitatory and inhibitory neurons. Nature *601*, 397–403.
35. Urban-Ciecko, J., and Barth, A.L. (2016). Somatostatin-expressing neurons in cortical networks. Nat. Rev. Neurosci. *17*, 401–409.
36. Hong, W., Kim, D.-W., and Anderson, D.J. (2014). Antagonistic control of social versus repetitive self-grooming behaviors by separable amygdala neuronal subsets. Cell *158*, 1348–1361.
37. Tasic, B., Yao, Z., Graybuck, L.T., Smith, K.A., Nguyen, T.N., Bertagnolli, D., Goldy, J., Garren, E., Economo, M.N., Viswanathan, S., et al. (2018). Shared and distinct transcriptomic cell types across neocortical areas. Nature *563*, 72–78.
38. Donega, V., Marcy, G., Lo Giudice, Q., Zweifel, S., Angonin, D., Fiorelli, R., Abrous, D.N., Rival-Gervier, S., Koehl, M., Jabaudon, D., and Raineteau, O. (2018). Transcriptional dysregulation in postnatal glutamatergic progenitors contributes to closure of the cortical neurogenic period. Cell Rep. *22*, 2567–2574.
39. Lee, W., Milewski, T.M., Dwortz, M.F., Young, R.L., Gaudet, A.D., Fonken, L.K., Champagne, F.A., and Curley, J.P. (2022). Distinct immune and transcriptomic profiles in dominant versus subordinate males in mouse social hierarchies. Brain Behav. Immun. *103*, 130–144.
40. Steffen, M.A., and Rehan, S.M. (2020). Genetic signatures of dominance hierarchies reveal conserved cis-regulatory and brain gene expression underlying aggression in a facultatively social bee. Genes Brain Behav. *19*, e12597.
41. McCann, K.E., Sinkiewicz, D.M., Rosenhauer, A.M., Beach, L.Q., and Huhman, K.L. (2019). Transcriptomic analysis reveals sex-dependent expression patterns in the basolateral amygdala of dominant and subordinate animals after acute social conflict. Mol. Neurobiol. *56*, 3768–3779.
42. Marowsky, A., Yanagawa, Y., Obata, K., and Vogt, K.E. (2005). A specialized subclass of interneurons mediates dopaminergic facilitation of amygdala function. Neuron *48*, 1025–1037.
43. Lin, D., Boyle, M.P., Dollar, P., Lee, H., Lein, E.S., Perona, P., and Anderson, D.J. (2011). Functional identification of an aggression locus in the mouse hypothalamus. Nature *470*, 221–226.
44. Williamson, C.M., Romeo, R.D., and Curley, J.P. (2017). Dynamic changes in social dominance and mPOA GnRH expression in male mice following social opportunity. Horm. Behav. *87*, 80–88.
45. Perez-Alcala, S., Nieto, M.A., and Barbas, J.A. (2004). LSox5 regulates RhoB expression in the neural tube and promotes generation of the neural crest. Development *131*, 4455-65.
46. Liu, S., Huang, L., Lin, Z., Hu, Y., Chen, R., Wang, L., and Shan, Y. (2017). RhoB induces the production of proinflammatory cytokines in TLR-triggered macrophages. Mol. Immunol. *87*, 200–206.
47. Maheu, M.E., Sharma, S., King, G., Maddox, S.A., Wingo, A., Lori, A., Michopoulos, V., Richardson, R., and Ressler, K.J. (2022). Amygdala DCX and blood Cdk14 are implicated as cross-species indicators of individual differences in fear, extinction, and resilience to trauma exposure. Mol. Psychiatry *27*, 956–966.
48. Choe, I.-H., Byun, J., Kim, K.K., Park, S., Kim, I., Jeong, J., and Shin, H.-S. (2017). Mice in social conflict show rule-observance behavior enhancing long-term benefit. Nat. Commun. *8*, 1176.
49. Coplan, J.D., Karim, A., Chandra, P., St. Germain, G., Abdallah, C.G., and Altemus, M. (2015). Neurobiology of maternal stress: role of social rank and central oxytocin in hypothalamic–pituitary adrenal axis modulation. Front. Psychiatry *6*, 100.
50. Colyn, L., Venzala, E., Marco, S., Perez-Otaño, I., and Tordera, R.M. (2019). Chronic social defeat stress induces sustained synaptic structural changes in the prefrontal cortex and amygdala. Behav. Brain Res. *373*, 112079.
51. Lang, F., and Cohen, P. (2001). Regulation and physiological roles of serum-and glucocorticoid-induced protein kinase isoforms. Sci. STKE *2001*, re17.
52. Tran, M.N., Maynard, K.R., Spangler, A., Huuki, L.A., Montgomery, K.D., Sadashivaiah, V., Tippani, M., Barry, B.K., Hancock, D.B., Hicks, S.C., et al. (2021). Single-nucleus transcriptome analysis reveals cell-type-specific molecular signatures across reward circuitry in the human brain. Neuron *109*, 3088–3103.e5.
53. Shimmura, T., Ohashi, S., and Yoshimura, T. (2015). The highest-ranking rooster has priority to announce the break of dawn. Sci. Rep. *5*, 11683.
54. Lun, A.T.L., Riesenfeld, S., Andrews, T., Dao, T.P., Gomes, T.; participants in the 1st Human Cell Atlas Jamboree, and Marioni, J.C. (2019). EmptyDrops: distinguishing cells from empty droplets in droplet-based single-cell RNA sequencing data. Genome Biol. *20*, 63.
55. Butler, A., Hoffman, P., Smibert, P., Papalexi, E., and Satija, R. (2018). Integrating single-cell transcriptomic data across different conditions, technologies, and species. Nat. Biotechnol. *36*, 411–420.
56. Korsunsky, I., Millard, N., Fan, J., Slowikowski, K., Zhang, F., Wei, K., Baglaenko, Y., Brenner, M., Loh, P.-R., and Raychaudhuri, S. (2019). Fast, sensitive and accurate integration of single-cell data with Harmony. Nat. Methods *16*, 1289–1296.
57. Van der Maaten, L., and Hinton, G. (2008). Visualizing data using t-SNE. J. Mach. Learn. Res. *9*, 2579–2605.
58. Camp, J.G., Sekine, K., Gerber, T., Loeffler-Wirth, H., Binder, H., Gac, M., Kanton, S., Kageyama, J., Damm, G., Seehofer, D., et al. (2017). Multilineage communication regulates human liver bud development from pluripotency. Nature *546*, 533–538.
59. Huang, D.W., Sherman, B.T., and Lempicki, R.A. (2009). Systematic and integrative analysis of large gene lists using DAVID bioinformatics resources. Nat. Protoc. *4*, 44–57.
60. Qiu, X., Mao, Q., Tang, Y., Wang, L., Chawla, R., Pliner, H.A., and Trapnell, C. (2017). Reversed graph embedding resolves complex single-cell trajectories. Nat. Methods *14*, 979–982.
61. Trapnell, C., Cacchiarelli, D., Grimsby, J., Pokharel, P., Li, S., Morse, M., Lennon, N.J., Livak, K.J., Mikkelsen, T.S., and Rinn, J.L. (2014). The dynamics and regulators of cell fate decisions are revealed by pseudotemporal ordering of single cells. Nat. Biotechnol. *32*, 381–386.
62. Wolf, F.A., Hamey, F.K., Plass, M., Solana, J., Dahlin, J.S., Göttgens, B., Rajewsky, N., Simon, L., and Theis, F.J. (2019). PAGA: graph abstraction reconciles clustering with trajectory inference through a topology preserving map of single cells. Genome Biol. *20*, 59.
63. Franceschini, A., Szklarczyk, D., Frankild, S., Kuhn, M., Simonovic, M., Roth, A., Lin, J., Minguez, P., Bork, P., Von Mering, C., and Jensen, L.J. (2013). STRING v9. 1: protein-protein interaction networks, with increased coverage and integration. Nucleic Acids Res. *41*, D808–D815.
64. Chin, C.-H., Chen, S.-H., Wu, H.-H., Ho, C.-W., Ko, M.-T., and Lin, C.-Y. (2014). cytoHubba: identifying hub objects and sub-networks from complex interactome. BMC Syst. Biol. *8*, S11.
65. Hu, X., Zhou, J., Zhang, Y., Zeng, Y., Jie, G., Wang, S., Yang, A., and Zhang, M. (2022). Identifying potential prognosis markers in hepatocellular carcinoma via integrated bioinformatics analysis and biological experiments. Front. Genet. *13*, 942454.
66. Bandettini, W.P., Kellman, P., Mancini, C., Booker, O.J., Vasu, S., Leung, S.W., Wilson, J.R., Shanbhag, S.M., Chen, M.Y., and Arai, A.E. (2012). MultiContrast Delayed Enhancement (MCODE) improves detection of subendocardial myocardial infarction by late gadolinium enhancement cardiovascular magnetic resonance: a clinical validation study. J. Cardiovasc. Magn. Reson. *14*, 83.
67. Bindea, G., Galon, J., and Mlecnik, B. (2013). CluePedia Cytoscape plugin: pathway insights using integrated experimental and in silico data. Bioinformatics *29*, 661–663.

STAR★METHODS

KEY RESOURCES TABLE

REAGENT or RESOURCE	SOURCE	IDENTIFIER
Biological samples		
Qingyuan Braised Chicken	Guangdong Tiannong Food Co., Ltd	N/A
Chemicals, peptides, and recombinant proteins		
Total RNA Extraction Reagent	Vazyme Biotech Co.,Ltd	Cat# 401
0.5M EDTA	Thermo Fisher Scientific	N/A
HiScript® III RT SuperMix for qPCR	Vazyme Biotech Co.,Ltd	Cat# R323
ChamQ Universal SYBR qPCR Master Mix	Vazyme Biotech Co.,Ltd	Cat# Q711
Software and algorithms		
Human amygdala single-cell data	Tran et al.[52]	https://libd-snrnaseq-pilot.s3.us-east-2.amazonaws.com/SCE_AMY-n5_tran-etal.rda
Monkey amygdala single-cell data	Zhang et al.[21]	https://www.ncbi.nlm.nih.gov/geo/query/acc.cgi?acc=GSE145765
Chicken amygdala single-cell data	This paper	the BioProject ID is PRJNA967858

RESOURCE AVAILABILITY

Lead contact

Further information and requests for resources and reagents should be directed to and will be fulfilled by the lead contact, Siyu Chen (chensiyu@fosu.edu.cn)).

Materials availability

This study did not generate new unique reagents.

Data and code availability

- Single-cell RNA-seq data have been deposited at GEO and are publicly available as of the date of publication. Accession number are listed in the key resources table.
- This paper does not report original code.
- Any additional information required to reanalyze the data reported in this paper is available from the lead contact upon request.

EXPERIMENTAL MODEL AND STUDY PARTICIPANT DETAILS

Method details

Animals and ethics

All animal experimentation was approved and performed according to procedures determined by the Laboratory Animal Welfare and Animal Experimental Ethical Inspection Committee of Foshan University. The guidelines of the experimental animal management of Foshan University were followed throughout the study, and the experimental protocols were approved by the Experimental Animal Care and Use Committee of Foshan University (Approval number: #Fosu202108). The experimental animals in this study were provided by Guangdong Tinoon's food company ltd.co. After the brooding period (at the age of 28 days), five Qingyuan partridge roosters in a group with six replicates, totally 30 individuals were entered into the experiment. They were reared under a conventional cage rearing system with the floor space allowance about 0.041 m^2 per chicken at day 70. The cages were located on the top tier of a three-tier battery cage building. For the convenience of individual identification, the two feet of each rooster were marked with different color rings.

Dominance hierarchy

Birds were deprived of food from 18:00 the day before the food competition test. At the age of 40, 50, 60 and 70 days, food competition test for ten minutes was conducted at 8:00 a.m., and the feeder was set to only allow one bird at a time to feed. The aggressive interactions (aggressive pecking, displacing, chasing and threatening), and both the winner and loser were recorded. From the record of the aggressive interactions, the dominance value of individual roosters was calculated by using the index of Clutton-Brock (ICB).[53] The formula was as follow:

Dominant value $= \frac{(B+\sum b+1)}{(L+\sum l+1)}$. Where B = number of individuals that a rooster beat; $\sum$b = total numbers that all rooters beat excluding the number of the subject itself; L = number of individuals that the rooster lost to; $\sum$l = total number that all roosters lost to excluding the subject itself. Accordingly, rank 1 (R1), R2, R3, R4, and R5 roosters with the descending order of the social rank were calculated.

Sample collection and preparation of single cell nucleus suspension

Amygdala tissue was isolated from the brain of 71 days old rooster and stored in liquid nitrogen for subsequent scRNA-seq. The preparation of single cell nucleus suspension, library construction, RNA sequencing and data analysis were completed by Guangzhou Genovo Biotechnology Co., Ltd. (Guangzhou, China). We mixed the amygdala tissues of high- and low social class (n = 6, in each) into a sample respectively to make a single nucleus suspension. To put it simply, the tissue homogenate was filtered with a 70 μm cell sieve, and a white nuclear layer would appear after adding Iohexol. After repeated cleaning, the tissue was filtered again with a 40 μm cell sieve. After centrifugation, 100 μL of nuclear cleaning solution was added to the supernatant to suspend the nucleus for precipitation. Then, a proper amount of single cell nucleus suspension was taken and mixed with 0.4% trypan blue dye solution at a ratio of 9:1, and then Countess ® II Automated Cell Counter counts cells was used, and the proportion of living cells was calculated. Ensure the proportion of living cells ≥ 90%, and adjust the cell concentration to 700-1200 nucleus/μL.

Single cell RNA sequencing

10X Genomics 5′ transcriptome uses short read long sequencing and microfluidic technology to achieve simultaneous transcriptome expression profile analysis of 500-10000 cells in each sample. The gel beads containing barcode information were combined with the mixture of cells and enzymes, and then wrapped by oil surfactant droplets located in the microfluidic "double cross" system to form GEMs (Gel Beads-In-Emulations). GEMs were flowed into the reservoir and collected. The gel beads dissolved and released barcode sequences, and then barcode sequence reversed transcribe cDNA fragments and labeled the samples. The gel beads and the oil drops were broken, and the cDNA was used as the template for PCR amplification. The products of all GEMs were mixed to construct a standard sequencing library. Then using the dual terminal sequencing mode of Illumina sequencing platform to conduct high-throughput sequencing on the constructed library. At the Read 1 end, 16 bp barcode information and 10 bp UMI information were included to determine cells and quantitate expression. At the end of Read 2, cDNA fragments were included for reference genome comparison to determine the gene corresponding to mRNA.

Quanlity control of sequencing data and quatification of gene expression

We used 10x Genomics official analysis software Cell Ranger to perform data quality statistics on the original data, and cell Ranger calls STAR (Spliced Transcripts Alignment to a Reference) comparison software to compare Read2 to the reference genome. According to the results of GTF annotation, the read on the comparison was classified as the read of exon, intron or intergenic region. In brief, the read of exon is classified as if at least 50% of a read was located in the exon region. If the reads were compared to a single exon region and one or more non exon regions, it was preferentially classified as an exon and its MAPQ was set to 255. Cell Ranger further aligned exon reads to the annotated transcript. If reads aligned to the exon of a transcript and the two directions were the same, it was considered to be aligned to the transcriptome, which was recorded as transcriptome reads. In the transcriptome reads, if only one gene was mapped by reads, they were considered to be uni mapped. Only uni-mapped reads can be used for UMI caching. Cell Ranger then filtered and corrected barcodes and UMIs. Cell barcodes were completely consistent with the known barcode sequence in the database. The expected number of cells was N. Arrange the barcodes according to the number of UMI counts from large to small, and take the first N barcodes. Record that the 99th percentile UMI count was m. Filter UMI count<m*10% barcode, and the remaining cells were valid. See the previous study for the determination of effective cell methods with low RNA content.[54]

Cell cluster analysis

Further quality control and analysis of single cell transcriptome data were performed with R package Seurat.[55] We filter cells according to the number of genes identified in a single cell (200-8000), the total number of UMI in a single cell (less than 50000), the proportion of mitochondrial gene expression in a single cell (less than 25%), the rate of multicellular and other indicators, and retain high-quality cells. Log homogenization was used to homogenize the expression amount. After removing low-quality cells, harmony was used for data consolidation and batch effect correction.[56] Then cell clustering analysis was carried out, and Euclidean distance between cells was calculated based on the previously determined principal components. Then, based on the euclidean distance between cells, the cells were embedded into the SNN (shared nearest neighbor) graph. Afterward, the SNN graph was divided into highly interconnected quasi populations according to the local adjacent JACCARD distance of two cells. Finally, louvain algorithm was used to cluster cells.[19] All cells in the single cell transcriptome were clustered into several cell subsets for the convenience of subsequent analysis. Cell subsets were visualized through t-SNE. The nonlinear dimensionality reduction method t-SNE was to map high-dimensional cell data into two-dimensional space, gather cells with similar expression patterns, separate cells with different expression patterns farther, and more intuitively show the differences between cells.[57]

Analysis of differentially expression genes (DEGs) in clusters

We used the rank sum test of seurat to analyze the differential gene expression of different cell subsets,[58] screen genes up-regulated and down regulated by the difference between groups. In each cell subpopulation were as follows: first, genes had to be at least 1.28-fold over-expressed in the target cluster. Second, genes had to be expressed in more than 25% of the cells belonging to the target cluster. Third,

p value is less than 0.01. Using DAVID biological information database,[59] the functional pathways representing each gene were analyzed from the GO database and KEGG public data. The threshold value was $p \leq 0.05$, and the GO term and path that meet this condition were those that significantly enriched in differentially expressed genes.

Pseudo time trajectory analysis

Monocle2 was used to analyze the pseudo chronological order of the differentiation of glutamate neurons, GABA neurons and oligodendrocytes.[60] Briefly, input the cell gene expression matrix into monocle, use monocle to reduce the data dimension to a two-dimensional plane, and then arrange the cells into a tree structure containing several branches and nodes to define these structures as different differentiation states. Based on the gene expression level of cells in different differentiation states, the genes differentially expressed with the differentiation state with the screening condition with FDR<1e-5 were screened.[61] Finally, according to the biological significance, the most primitive cell group in the differentiation state was defined as the cell group with the smallest pseudo time in the cell trajectory, and the pseudo time value of all cells was calculated. Based on the pseudo time value, monocle modeled the gene expression level as a smooth and nonlinear quasi time function, to verify the change of gene expression accompanied by the change of the pseudo time value. We screened genes with FDR<1e-5 as differential genes.

The partition based graph abstraction (PAGA) was used to analyze the differentiation trajectory of oligodendrocytes, which was a method for studying cell differentiation based on single cell transcriptome data.[62] It constructed differentiation tubes between cell subpopulations according to cell atlas, which retained the continuity of high-dimensional data to the greatest extent. The PAGA graph was made using the preprocessed Seurat object. The Scanpy (v1.6.0) function scanpy.pp. neighbors was ran using the PCA embeddings calculated by Seurat. Then, scanpy.tl.paga was ran using Seurat clusters as groups and finally the plot was generated using the function sc.pl.paga_compare. The Rfast2 software package was used to perform correlation statistics and significance calculations for each gene. We identified significantly differential expression genes with FDR<1e-7 on the pseudo-time axis.

Protein-protein interaction (PPI) network construction and identification of hub genes

We used the string v9 protein interaction network database to find the corresponding proteins of marker genes in the database through blast comparison, and took the relevant network relationship of corresponding proteins as the relevant network relationship of marker genes. After obtaining the protein interaction relationship information of the marker gene, the result file into Cytoscape for network visualization was imported.[63] Then the CytoHubba application in Cytoscape was used to identify hub genes. CytoHubba with 11 different algorithms can be sorted nodes in the network according to network characteristics.[64] According to the analysis results, relevant genes with MNC (Maximum Neighborhood Component), EPC (Edge percolored component), Closeness (Node connect closeness), Degree (Node connect degree), and MCC (Maximum clique centrality) greater than or equal to 20 were screened for further analysis.[65] Then, the MCODE plug-in of Cytoscape species was used to screen important gene modules in the molecular interaction visualization network.[66] The gene modules were further sorted according to the network score. The module with the highest score was an important gene module. We selected the module with the highest score for further verification and analysis and identified the genes co-expressed by five algorithms in CytoHubba and those in MCODE with the highest score as HUB genes. In addition, we used ClueGo and Cluepedia plug-ins in Cytoscape to perform GO analysis and visualization of MCODE modules.[67]

Cross species data analysis

Two amygdala single-cell datasets of human[52] and rhesus monkey[21] were downloaded for interspecies comparison. The 'biomart' in the R package converts the genes of human and rhesus monkey into chicken homologous genes, and only homologous genes in all three species were retained for analysis. Clustering was performed using the 'Seurat' method mentioned above, visualizing the dimensionality reduction clustering of three species, and outputting the upregulated genes of each subgroup for subgroup identification. Based on the recognition results of cell subgroups, proportion of cells in each subgroup to the total cells was calculated, and the cloud tool of the 'omicshare platform' was used to draw a rive map (https://www.omicshare.com/tools/Home/Soft/getsoft). The integrated data was used to build evolutionary tree, and the expression amount of each sample was calculated, the distance matrix was calculated with the 'dist' function in R package, the hierarchical clustering was carried out by 'hclust', and the evolution tree was derived by 'itol'.

RNA extraction and quantitative real time PCR (qRT-PCR)

The expressions of hub genes of amygdala from the highest and lowest social rank individuals (n = 6, in each) were determined. The qRT-PCR analysis was set up three biologicals. The total RNA of tissues was extracted with Total RNA extraction Reagent (R401-01) according to manufacturer's method. For qRT-PCR, the extracted RNA (500ng) was used to synthesize cDNA using a reverse transcription kit (R323-01). qRT-PCR was performed in the Applied Biosystems ™ QuantStudio ™ (Thermo Fisher Scientific) using ChamQTM® SYBR qPCR Green Master Mix kits (Q711-02). All kits were purchased from Vazyme Biotech Co., Ltd (Nanjing, China). The relative gene expression was analyzed by $2^{-\Delta Ct}$ of the internal reference gene GAPDH. The primers of were designed by Primer3web version 4.1.0 (https://primer3.ut.ee/), and the primers used were listed in Table S5.